

Kinetic Interacting Particle Langevin Monte Carlo

Paul Felix Valsecchi Oliva and O. Deniz Akyildiz

Department of Mathematics, Imperial College London

[paul.valsecchi-oliva21, deniz.akyildiz@imperial.ac.uk](mailto:paul.valsecchi-oliva21,deniz.akyildiz@imperial.ac.uk)

April 17, 2026

Abstract

This paper introduces and analyses interacting underdamped Langevin algorithms, termed Kinetic Interacting Particle Langevin Monte Carlo (KIPLMC) methods, for statistical inference in latent variable models. We propose a diffusion process that evolves jointly in the space of parameters and latent variables and show that the stationary distribution of this diffusion concentrates around the maximum marginal likelihood estimate of the parameters. We then provide two explicit discretisations of this diffusion as practical algorithms to estimate parameters of statistical models. For each algorithm, we obtain nonasymptotic rates of convergence in Wasserstein-2 distance for the case where the joint log-likelihood is strongly concave with respect to latent variables and parameters. We achieve accelerated convergence rates clearly demonstrating improvement in dimension dependence. To demonstrate the utility of the introduced methodology, we provide numerical experiments that illustrate the effectiveness of the proposed diffusion for statistical inference. Our setting covers a broad number of applications, including unsupervised learning, statistical inference, and inverse problems.

1 Introduction

Latent variable models (LVMs) are ubiquitous in many areas of statistical science, e.g., complex probabilistic models for text, audio, video and images [9, 49, 29], or inverse problems [28]. These models capture the underlying structure of the data in terms of low-dimensional variables – a structure that often exists in real world [52]. However, LVMs often require non-trivial procedures for their estimation as their likelihood is often intractable.

Consider a generic latent variable model as $p_\theta(x, y)$, parameterised by $\theta \in \mathbb{R}^{d_\theta}$, for *fixed*, observed data $y \in \mathbb{R}^{d_y}$, and latent variables $x \in \mathbb{R}^{d_x}$. Thus, formally, we see the statistical model as a real-valued mapping $p_\theta(x, y) : \mathbb{R}^{d_x} \times \mathbb{R}^{d_\theta} \rightarrow \mathbb{R}$. The task we are interested in is to estimate the parameter θ that explains the fixed dataset y . Often, this is achieved via the maximum likelihood estimation (MLE). In our setting, due to the presence of latent variables, we aim at finding the maximum *marginal* likelihood estimation (MMLE), which is termed the MMLE problem [22]. More precisely, our problem takes the form

$$\bar{\theta}_* \in \operatorname{argmax}_{\theta \in \mathbb{R}^{d_\theta}} \log p_\theta(y), \quad (1)$$

where $p_\theta(y) := \int p_\theta(x, y) dx$ is the *marginal likelihood* (also called the model evidence in Bayesian statistics [7]). It is apparent from (1) that the problem cannot be solved via optimisation techniques alone for most statistical models.

Classically, this problem is solved with the iterative expectation maximisation (EM) algorithm [22], which provably converges to a local maximum. At a given parameter estimate θ_n , the EM algorithm implements a map $\theta_n \mapsto \operatorname{argmax}_{\theta \in \mathbb{R}^{d_\theta}} \mathbb{E}_{p_{\theta_n}(x|y)}[\log p_\theta(x, y)]$, which is guaranteed to increase the marginal likelihood at

each iteration. This procedure requires an ‘‘E-step’’, namely the computation (or estimate) of the expectation w.r.t. the posterior distribution of the latent variables $p_{\theta_n}(x|y)$, and an ‘‘M-step’’, which is the maximisation of the expected log-likelihood w.r.t. θ . These steps are intractable in general and can be approximated with a variety of methods, which have been extensively explored. For example, Monte Carlo EM [50] and stochastic EM [13] have been widely studied [14, 15, 48, 10, 11, 23].

In the most general case, the EM algorithm is implemented using Markov chain Monte Carlo (MCMC) techniques for the E-step [6], and numerical optimisation techniques for the M-step [40, 38, 36]. With the popularity of unadjusted Langevin algorithm (ULA) in Bayesian statistics and machine learning [24, 25, 18], novel variants of EM algorithms use unadjusted chains. Most notably, De Bortoli et al. [21] studied an algorithm termed Stochastic Optimisation via Unadjusted Langevin (SOUL), which performs unadjusted Langevin steps for the E-step and stochastic gradient ascent for the M-step, building on the ideas of Atchadé et al. [6]. In the MCMC based EM setting, the bias incurred finite MCMC steps complicates the theoretical analysis and requires stringent conditions for step-sizes.

An alternative approach was developed in Kuntz et al. [35] where the authors proposed an interacting particle system, consisting of N particles to replace sequential MCMC steps. This framework, termed particle gradient descent (PGD), is based on the idea of joint optimisation and sampling to avoid a double-loop structure as in MCMC-based approaches, which results in an efficient algorithmic framework as well as one that is amenable to theoretical analysis Caprio et al. [12]. Inspired by the approach in Kuntz et al. [35], a closely related interacting particle system was proposed in Akyildiz et al. [3], where a scaled noise is injected in the θ -dimension. The authors termed this method interacting particle Langevin algorithm (IPLA) and proved error bounds for the algorithm. This seemingly small modification is significant, making the algorithm an instance of a Langevin diffusion (an observation we build on in this paper), streamlining the theoretical analysis and opening the door to a wide variety of extensions with theoretical guarantees. The IPLA methodology has been already utilised in other contexts, see, Johnston et al. [33] for superlinear extensions and Cordero-Encinar et al. [17] for a set of proximal methods based on IPLA, and Akyildiz et al. [2] for relations between IPLA and multiscale methods.

Contributions. In this paper, we develop optimisation methods for MMLE based on underdamped Langevin samplers. Our contributions can be summarised as follows:

(C1) We propose the kinetic interacting particle Langevin diffusion (KIPLD), a diffusion process to optimise the marginal likelihood in latent variable models. We prove that the stationary measure of this diffusion concentrates around the MMLE (Propositions 1 and 2) and the KIPLD converges to this measure exponentially fast (Proposition 3).

(C2) We then develop our first kinetic interacting particle Langevin Monte Carlo (KIPLMC) method, termed KIPLMC1 – an exponential integrator discretisation of KIPLD. We prove discretisation error bounds for our method showing convergence rates in both time and step-size (Theorem 1), closing the problem of nonasymptotic analysis of this method in the strongly convex case. In particular, we show that KIPLMC1 attains accelerated rates of convergence compared to its overdamped counterparts IPLA [3] and PGD [12]. While these overdamped diffusion-based MMLE methods achieve an ε error in Wasserstein-2 distance in $\tilde{\mathcal{O}}(d_x \varepsilon^{-2})$ steps, we prove that KIPLMC1 attains ε error in $\tilde{\mathcal{O}}(\sqrt{d_x} \varepsilon^{-1})$ steps.

(C3) We then introduce a splitting-based explicit discretisation scheme within this setting, which leads to a novel MMLE algorithm, termed KIPLMC2. We study the nonasymptotic behaviour of this method (Theorem 2), showing that the algorithm obtains an error ε in Wasserstein-2 distance in $\tilde{\mathcal{O}}(\sqrt{d_x d_\theta} \varepsilon^{-2})$ steps.

(C4) Finally, we provide solid empirical evidence of the performance of our methods in a variety of settings, including synthetic and realistic models. In the convex setting, we validate the $\mathcal{O}(N^{-1/2})$ concentration onto the maximiser θ_\star and demonstrate the increased stability of the momentum-based methods. In the non-convex setting, we show the acceleration of the proposed methods, as well as the importance of the choice

of numerical integrator, validating our methodological contribution.

Relations to existing work. The KIPLD is similar to the continuous time system on which the momentum particle gradient descent (MPGD) algorithm by Lim et al. [37] is based (see Eq. (21) in Lim et al. [37] where we take $\eta_\theta = \eta_x = 1$ and $\gamma_x = \gamma_\theta = \gamma$). In line with the work done by Akyildiz et al. [3], we inject the θ -dynamics with an appropriately scaled Brownian motion, i.e., $\sqrt{2\gamma/N}d\mathbf{B}_t^0$. The advantage of studying and implementing this version is due to the fact that the new system can be shown to be an example of a standard underdamped Langevin diffusion, which enables us to show non-asymptotic bounds in a streamlined manner. Furthermore, our discretisations differ from the MPGD routine: the KIPLMC1 algorithm does not use a gradient correction step, whilst KIPLMC2 is based on a different integrator. In Sec. 5, we show that these algorithms obtain similar stability, while having theoretical guarantees.

The paper is structured as follows. In Section 2, we present the background work on underdamped Langevin diffusions for sampling and interacting particle systems for the MMLE problem. Following this introduction, in Section 3, we present a new diffusion targeting the solution of the MMLE problem and present the associated algorithms KIPLMC1 and KIPLMC2. Section 4 presents the nonasymptotic analysis of KIPLMC methods, providing a clear evidence of improved theoretical bounds due to the acceleration. Finally, in Section 5, we present a variety of experiments to support our theoretical findings.

Notation

Let $\mathcal{P}(\mathbb{R}^d)$, for $d \geq 1$, denote the set of probability measures on $(\mathbb{R}^d, \mathcal{B}(\mathbb{R}^d))$, where $\mathcal{B}(\mathbb{R}^d)$ is the Borel σ -algebra. We write $\langle \cdot, \cdot \rangle$ and $\|\cdot\|$ for the Euclidean inner product and norm on \mathbb{R}^d . We also use $[N] = \{1, \dots, N\}$ and \mathbb{N} for the positive integers. For $p > 0$, define the Wasserstein- p distance by

$$W_p(\pi, \nu) = \left(\inf_{\Gamma \in \mathbf{T}(\pi, \nu)} \int_{\mathbb{R}^d \times \mathbb{R}^d} \|x - y\|_p^p d\Gamma(x, y) \right)^{1/p}$$

where $\mathbf{T}(\pi, \nu)$ is the set of couplings on $\mathbb{R}^d \times \mathbb{R}^d$.

We also define $\tilde{\mathcal{O}}$ as the big \mathcal{O} notation, up to logarithmic orders.

2 Technical Background

Before presenting our proposed diffusion and algorithms, we introduce some concepts that will be useful to us in this paper. We first introduce the kinetic Langevin diffusion and its associated algorithms, which are the building blocks of our proposed methods. Then, we present the IPLA algorithm, which is the closest method to our proposed algorithms and serves as a starting point for our developments.

2.1 Kinetic Langevin Monte Carlo

In recent years, the Langevin diffusion and its associated algorithms have been widely used in statistics and machine learning to sample from complex distributions. The overdamped Langevin diffusion is given by the stochastic differential equation (SDE)

$$d\mathbf{Z}_t = -\nabla U(\mathbf{Z}_t)dt + \sqrt{2}d\mathbf{B}_t, \tag{2}$$

where $U : \mathbb{R}^d \rightarrow \mathbb{R}$ is a potential function and $(\mathbf{B}_t)_{t \geq 0}$ is a Brownian motion. Under certain regularity conditions, this system is known to be invariant w.r.t. the measure $\pi(dz) \propto \exp(-U(z))dz$ [43]. Under the strongly convex and Lipschitz-gradient setting, a standard Euler-Maruyama discretisation of this diffusion, called ULA, is known to attain at most $\mathcal{O}(\varepsilon)$ error in Wasserstein-2 distance to the stationary measure in $\tilde{\mathcal{O}}(d\varepsilon^{-2})$ steps [18, 25].

An alternative to the *overdamped* Langevin diffusions given in (2), is another class of diffusions called *underdamped* Langevin diffusions [43]. This class of diffusions is akin to second-order differential equations

and defined over position and momentum variables. In particular, for a d -dimensional target measure $\pi(dz) \propto \exp(-U(z))dz$, the underdamped (kinetic) Langevin diffusion is given by the SDE

$$\begin{aligned} d\mathbf{Z}_t &= \mathbf{V}_t dt \\ d\mathbf{V}_t &= -\gamma \mathbf{V}_t dt - \nabla_z U(\mathbf{Z}_t) dt + \sqrt{2\gamma} d\mathbf{B}_t, \end{aligned} \tag{3}$$

where $\gamma > 0$ is called the friction coefficient and $(\mathbf{B}_t)_{t \geq 0}$ is a Brownian motion. Under certain regularity conditions [43], this system is known to be invariant w.r.t. an extended stationary measure of the form

$$\bar{\pi}(dz, dv) \propto \exp\left(-U(z) - \frac{1}{2}\|v\|^2\right) dz dv. \tag{4}$$

This means that we can recover the samples from our target measure $\pi(dz) \propto \exp(-U(z))dz$ by sampling from (4) and then marginalising out the velocity variable.

The structure in (3) allows for smoother sample paths and faster convergence to the stationary measure compared to the overdamped case [16]. This has motivated the development of algorithms based on discretisations of the underdamped Langevin diffusion, termed kinetic Langevin Monte Carlo (KLMC) [20]. These methods have been shown to achieve improved convergence rates compared to their overdamped counterparts, making them a competitive alternative for sampling from complex distributions. In particular, under the strongly convex and Lipschitz-gradient setting, KLMC is known to attain at most $\mathcal{O}(\varepsilon)$ error in Wasserstein-2 distance to the stationary measure in $\tilde{\mathcal{O}}(\sqrt{d\varepsilon^{-1}})$ steps [20]. In this paper, we build on the framework of KLMC methods to develop algorithms for the MMLE problem.

2.2 MMLE via Interacting Particle Langevin Algorithm

Consider the MMLE problem given in (1), that is, to find the parameter θ that maximises the marginal likelihood $p_\theta(y)$. As summarised in the introduction, this problem is often solved with the EM algorithm, typically implemented with a double-loop structure consisting of MCMC techniques for the E-step and numerical optimisation techniques for the M-step [6, 21].

In contrast to this approach, Kuntz et al. [35] propose an interacting particle system, the particle gradient descent (PGD) algorithm, to approximate the gradient of the θ -dynamics by running independent particles to integrate out latent variables. Inspired by this, Akyildiz et al. [3] attempt to solve the MMLE problem with a similar system, termed the interacting particle Langevin algorithm (IPLA), which is a modification of PGD where θ -dynamics contain a carefully scaled noise. This approach produces a system that is akin to the ULA and makes the theoretical analysis streamlined using the analysis produced for ULA [18, 25]. The proposed algorithm is a discretisation of a system of interacting Langevin SDEs which evolves in $\mathbb{R}^{d_\theta} \times \mathbb{R}^{Nd_x}$ where N distinct particles are retained for latent variables. More precisely, IPLA recursions are based on the SDE:

$$d\boldsymbol{\theta}_t = -\frac{1}{N} \sum_{i=1}^N \nabla_\theta U(\boldsymbol{\theta}_t, \mathbf{X}_t^i) dt + \sqrt{\frac{2}{N}} d\mathbf{B}_t^0, \tag{5}$$

$$d\mathbf{X}_t^i = -\nabla_x U(\boldsymbol{\theta}_t, \mathbf{X}_t^i) dt + \sqrt{2} d\mathbf{B}_t^i, \tag{6}$$

for $i \in [N]$, where $(\mathbf{B}_t^0)_{t \geq 0}$ is a Brownian motion evolving on \mathbb{R}^{d_θ} and $(\mathbf{B}_t^i)_{t \geq 0}$ for $i \in [N]$ are Brownian motions evolving on \mathbb{R}^{d_x} . In this case, Akyildiz et al. [3] observe that the θ -marginal of the stationary measure of this system takes the form $\pi_\Theta(d\theta) \propto \exp(N \log p_\theta(y)) d\theta$ which concentrates on the MMLE $\hat{\theta}_*$ as N grows, where N plays the role of inverse temperature [31]. The authors then identify the convergence rate to the joint stationary measure, as well as an error bound for the discretisation error, from which an error can be determined between the θ -iterate of the algorithm and the MMLE.

3 Kinetic Interacting Particle Langevin Monte Carlo

To develop our methodology, we start with the following diffusion process:

$$\begin{aligned}
d\boldsymbol{\theta}_t &= \mathbf{V}_t^\theta dt \\
d\mathbf{X}_t^i &= \mathbf{V}_t^{x_i} dt, \\
d\mathbf{V}_t^\theta &= -\gamma \mathbf{V}_t^\theta dt - \frac{1}{N} \sum_{i=1}^N \nabla_\theta U(\boldsymbol{\theta}_t, \mathbf{X}_t^i) dt + \sqrt{\frac{2\gamma}{N}} d\mathbf{B}_t^0 \\
d\mathbf{V}_t^{x_i} &= -\gamma \mathbf{V}_t^{x_i} dt - \nabla_x U(\boldsymbol{\theta}_t, \mathbf{X}_t^i) dt + \sqrt{2\gamma} d\mathbf{B}_t^i,
\end{aligned} \tag{KIPLD}$$

for $i \in [N]$, where $\{(\mathbf{B}_t^i)_{t \geq 0}\}_{i \in [N]}$ is a family of \mathbb{R}^{d_x} -valued Brownian motions and $(\mathbf{B}_t^0)_{t \geq 0}$ is an \mathbb{R}^{d_θ} -valued Brownian motion. This diffusion has the property that its θ -marginal at stationarity concentrates around the global minimisers of $\log p_\theta(y)$ (see Section 4).

Next, we introduce two numerical integrators for the KIPLD: firstly, we consider an Exponential Integrator, as discussed in Dalalyan and Riou-Durand [20]; secondly, a splitting scheme is applied, as described in Monmarché [41].

3.1 Exponential Integrator (KIPLMC1)

In order to derive the exponential integrator discretisation of KIPLD, following Dalalyan and Riou-Durand [20], we begin by defining the functions

$$\psi_0^t = e^{-\gamma t}, \quad \psi_1^t = \int_0^t e^{-\gamma s} ds = \frac{1}{\gamma}(1 - e^{-\gamma t}), \quad \psi_2^t = \int_0^t \psi_1^s ds = \frac{1}{\gamma^2}(e^{-\gamma t} - 1) + \frac{t}{\gamma}.$$

The exponential integrator is obtained by freezing the nonlinear drift terms $\nabla_\theta U(\boldsymbol{\theta}_t, X_t^i)$ and $\nabla_x U(\boldsymbol{\theta}_t, X_t^i)$ at the beginning of each time step and solving exactly the resulting linear stochastic differential equation.

More precisely, let $t_n = n\eta$. Over the interval $[t_n, t_{n+1}]$ we approximate the dynamics (KIPLD) by freezing the gradients at $(\boldsymbol{\theta}_n, X_n^i)$,

$$F_n^\theta = \frac{1}{N} \sum_{i=1}^N \nabla_\theta U(\boldsymbol{\theta}_n, X_n^i), \quad F_n^{x_i} = \nabla_x U(\boldsymbol{\theta}_n, X_n^i),$$

which yields the linear system

$$\begin{aligned}
d\boldsymbol{\theta}_t &= \mathbf{V}_t^\theta dt, \\
d\mathbf{X}_t^i &= \mathbf{V}_t^{x_i} dt, \\
d\mathbf{V}_t^\theta &= -\gamma \mathbf{V}_t^\theta dt - F_n^\theta dt + \sqrt{\frac{2\gamma}{N}} d\mathbf{B}_t^0, \\
d\mathbf{V}_t^{x_i} &= -\gamma \mathbf{V}_t^{x_i} dt - F_n^{x_i} dt + \sqrt{2\gamma} d\mathbf{B}_t^i,
\end{aligned}$$

for $i \in [N]$, with initial condition

$$(\boldsymbol{\theta}_{t_n}, \mathbf{X}_{t_n}^i, \mathbf{V}_{t_n}^\theta, \mathbf{V}_{t_n}^{x_i}) = (\boldsymbol{\theta}_n, X_n^i, V_n^\theta, V_n^{x_i}).$$

Since the system is linear with constant coefficients, it can be solved explicitly. Using an integrating factor for the velocity equation gives, for $s \in [0, \eta]$,

$$\begin{aligned}
V_{t_n+s}^\theta &= \psi_0^s V_n^\theta - \psi_1^s F_n^\theta + \sqrt{\frac{2\gamma}{N}} \int_0^s \psi_0^{s-\tau} d\mathbf{B}_{t_n+\tau}^0, \\
V_{t_n+s}^{x_i} &= \psi_0^s V_n^{x_i} - \psi_1^s F_n^{x_i} + \sqrt{2\gamma} \int_0^s \psi_0^{s-\tau} d\mathbf{B}_{t_n+\tau}^i.
\end{aligned}$$

Integrating once more yields the updates for the positions

$$\begin{aligned}\theta_{t_n+s} &= \theta_n + \psi_1^s V_n^\theta - \psi_2^s F_n^\theta + \sqrt{\frac{2\gamma}{N}} \int_0^s \psi_1^{s-\tau} d\mathbf{B}_{t_n+\tau}^0, \\ X_{t_n+s}^i &= X_n^i + \psi_1^s V_n^{x_i} - \psi_2^s F_n^{x_i} + \sqrt{2\gamma} \int_0^s \psi_1^{s-\tau} d\mathbf{B}_{t_n+\tau}^i.\end{aligned}$$

Evaluating these expressions at $s = \eta$ gives the one-step update of the discretised process. The stochastic integrals appearing above are jointly Gaussian random variables. For each $i \in \{0, \dots, N\}$ we define

$$\varepsilon_n^i = \int_0^\eta \psi_0^{\eta-s} dB_{t_n+s}^i, \quad \varepsilon_n^{i,\prime} = \int_0^\eta \psi_1^{\eta-s} dB_{t_n+s}^i.$$

Now note that $(\varepsilon_n^0, \varepsilon_n^{0,\prime}) \in \mathbb{R}^{d_\theta} \times \mathbb{R}^{d_\theta}$ and $(\varepsilon_n^i, \varepsilon_n^{i,\prime}) \in \mathbb{R}^{d_x} \times \mathbb{R}^{d_x}$ for $i = 1, \dots, N$. Consider each coordinate of these pairs:

$$\varepsilon_{n,j}^i = \int_0^\eta \psi_0^{\eta-s} dB_{t_n+s,j}^i, \quad \varepsilon_{n,j}^{i,\prime} = \int_0^\eta \psi_1^{\eta-s} dB_{t_n+s,j}^i.$$

For every (i, j) , using Itô isometry [42], we can obtain $C = \text{Cov}(\varepsilon_{n,j}^i, \varepsilon_{n,j}^{i,\prime})$ as

$$C = \int_0^\eta \begin{pmatrix} (\psi_0^t)^2 & \psi_0^t \psi_1^t \\ \psi_0^t \psi_1^t & (\psi_1^t)^2 \end{pmatrix} dt. \quad (7)$$

We note that $C \in \mathbb{R}^{2 \times 2}$ and denote its Cholesky decomposition by $C = LL^\top$. Hence the Gaussian pair

Algorithm 1 KIPLMC1

Require: $\gamma, \eta > 0$, $N, M \in \mathbb{N}$

- 1: Compute the covariance matrix C given in (7) and its Cholesky decomposition $C = LL^\top$.
- 2: Draw $\theta_0, X_0^i, V_0^\theta, V_0^{x_i}$, for $i \in [N]$
- 3: **for** $n = 0 : M - 1$ **do**
- 4: Draw: $\xi_n^i, \xi_n^{i,\prime}$ from a standard Gaussian (in \mathbb{R}^{d_θ} for $i = 0$ and \mathbb{R}^{d_x} otherwise)

$$\varepsilon_n^i = L_{11}\xi_n^i, \quad \varepsilon_n^{i,\prime} = L_{21}\xi_n^i + L_{22}\xi_n^{i,\prime}$$

for $i = 0, \dots, N$ where ξ_n^0 and $\xi_n^{0,\prime}$ are standard d_x and d_θ dimensional Normal random variables.

- 5: Compute the average gradient of the potential:

$$F_n^\theta = \frac{1}{N} \sum_{i=1}^N \nabla_\theta U(\theta_n, X_n^i), \quad F_n^{x_i} = \nabla_x U(\theta_n, X_n^i).$$

Update the parameters, particles and their momenta:

$$\begin{aligned}\theta_{n+1} &= \theta_n + \psi_1^\eta V_n^\theta - \psi_2^\eta F_n^\theta + \sqrt{\frac{2\gamma}{N}} \varepsilon_n^{0,\prime} \\ X_{n+1}^i &= X_n^i + \psi_1^\eta V_n^{x_i} - \psi_2^\eta F_n^{x_i} + \sqrt{2\gamma} \varepsilon_n^{i,\prime} \\ V_{n+1}^\theta &= \psi_0^\eta V_n^\theta - \psi_1^\eta F_n^\theta + \sqrt{\frac{2\gamma}{N}} \varepsilon_n^0 \\ V_{n+1}^{x_i} &= \psi_0^\eta V_n^{x_i} - \psi_1^\eta F_n^{x_i} + \sqrt{2\gamma} \varepsilon_n^i\end{aligned} \quad (\text{KIPLMC1})$$

for $i \in [N]$.

- 6: Output: $(\theta_M, X_M^1, \dots, X_M^N)$
-

$(\varepsilon_{n,j}^i, \varepsilon_{n,j}^{i'})$ can be sampled by setting

$$\begin{pmatrix} \varepsilon_{n,j}^i \\ \varepsilon_{n,j}^{i'} \end{pmatrix} = L \begin{pmatrix} \xi_{n,j}^i \\ \xi_{n,j}^{i'} \end{pmatrix},$$

where $\xi_{n,j}^i$ and $\xi_{n,j}^{i'}$ are independent standard Gaussian random variables.

Substituting these expressions for $s = \eta$ yields the KIPLMC1 scheme. The full algorithm is given in Algorithm 1 and a more explicit derivation in Appendix B.

3.2 A Splitting Scheme (KIPLMC2)

We next introduce KIPLMC2, an adaptation of the underdamped Langevin sampler introduced by Horowitz [30] and extensively studied by Monmarché [41]. This splitting scheme is termed OBABO and it is a second order scheme, only requiring the first order derivatives of U . The idea is to split the numerical scheme into simpler subflows that can be solved explicitly. More precisely, in our KIPLD case, we decompose the flow into a Ornstein-Uhlenbeck step (O), a velocity drift step (B) and a particle update step (A).

Algorithm 2 KIPLMC2 Algorithm

Require: $\gamma, \eta > 0, N, M \in \mathbb{N}$

- 1: Draw $\theta_0, X_0^i, V_0^\theta, V_0^{x_i}$, for $i \in [N]$
- 2: **for** $n = 0 : M - 1$ **do**
- 3: Draw $\varepsilon_n, \varepsilon_n'$ from $d_\theta + Nd_x$ -dimensional Gaussians and for $i \in [N]$,
- 4: Compute the gradients of the potential:

$$F_n^\theta = \frac{1}{N} \sum_{i=1}^N \nabla_\theta U(\theta_n, X_n^i), \quad F_n^{x_i} = \nabla_x U(\theta_n, X_n^i).$$

- 5: Update the momenta via (O)+(B) steps:

$$\begin{aligned} V_{n+\frac{1}{2}}^\theta &= \delta V_n^\theta + \sqrt{\frac{1-\delta^2}{N}} \xi_n^\theta - \frac{\eta}{2} F_n^\theta, \\ V_{n+\frac{1}{2}}^{x_i} &= \delta V_n^{x_i} + \sqrt{1-\delta^2} \xi_n^{x_i} - \frac{\eta}{2} F_n^{x_i}, \end{aligned}$$

- 6: Update parameters and particles via (A):

$$\theta_{n+1} = \theta_n + \eta V_{n+\frac{1}{2}}^\theta, \quad X_{n+1}^i = X_n^i + \eta V_{n+\frac{1}{2}}^{x_i},$$

for $i \in [N]$.

- 7: Re-compute the gradient potentials

$$F_{n+1}^\theta = \frac{1}{N} \sum_{i=1}^N \nabla_\theta U(\theta_{n+1}, X_{n+1}^i), \quad F_{n+1}^{x_i} = \nabla_x U(\theta_{n+1}, X_{n+1}^i).$$

- 8: Update the momenta via the (B)+(O) steps:

$$\begin{aligned} V_{n+1}^\theta &= \delta V_{n+\frac{1}{2}}^\theta - \frac{\delta\eta}{2} F_{n+1}^\theta + \sqrt{\frac{1-\delta^2}{N}} \xi_n^{\theta'}, \\ V_{n+1}^{x_i} &= \delta V_{n+\frac{1}{2}}^{x_i} - \frac{\delta\eta}{2} F_{n+1}^{x_i} + \sqrt{1-\delta^2} \xi_n^{x_i'}, \end{aligned}$$

for $i \in [N]$.

return θ_M

In the OBABO case, over a full time-step η , the (O) step is applied over a $\eta/2$ half-step, the (B) step is also applied to a $\eta/2$ half-step, (A) is applied as a full time-step η , followed by a reversed application of (B) and (O) for half-steps. We denote these intermediate time-steps by $n + \frac{1}{4}$, $n + \frac{1}{2}$ and $n + \frac{3}{4}$, though we note that these time-steps do not correspond to simulated time. The order in which these steps are taken is critical [41] and in our case we will limit ourselves to considering the OBABO ordering.

More precisely, the Ornstein-Uhlenbeck half-step (O) flow is given as

$$\begin{aligned} d\mathbf{V}_t^\theta &= -\gamma \mathbf{V}_t^\theta dt + \sqrt{\frac{2\gamma}{N}} d\mathbf{B}_t^0, \\ d\mathbf{V}_t^{x_i} &= -\gamma \mathbf{V}_t^{x_i} dt + \sqrt{2\gamma} d\mathbf{B}_t^i, \end{aligned}$$

over the time-interval $[t_n, t_{n+1/2}]$, for $i \in [N]$, where the parameters θ_t and \mathbf{X}_t^i are frozen and we initialise at $(\mathbf{V}_{n\eta}^\theta, \mathbf{V}_{n\eta}^{x_i}) = (V_n^\theta, V_n^{x_i})$. Using the classic analytic solution to the Ornstein-Uhlenbeck equation and the Itô Isometry we obtain,

$$\begin{aligned} V_{n+\frac{1}{4}}^\theta &= \delta V_n^\theta + \frac{1}{\sqrt{N}} \sqrt{1 - \delta^2} \xi_n^0, \\ V_{n+\frac{1}{4}}^{x_i} &= \delta V_n^{x_i} + \sqrt{1 - \delta^2} \xi_n^i, \end{aligned} \tag{O}$$

with $\delta = e^{-\eta\gamma/2}$ and i.i.d. standard Gaussians ξ_n^0 and ξ_n^i , in \mathbb{R}^{d_θ} and \mathbb{R}^{d_x} , respectively.

The momentum drift update (B) updates V^θ and V^{x_i} with the first order Taylor scheme for the integrals of $N^{-1} \sum_{i=1}^N \nabla_\theta U(\theta, X^i)$ and $\nabla_{x_i} U(\theta, X^i)$, i.e. we consider the flow to be given as

$$\begin{aligned} d\mathbf{V}_t^\theta &= -F_n^\theta dt, \\ d\mathbf{V}_t^{x_i} &= -F_n^{x_i} dt, \end{aligned}$$

over $t \in [t_n, t_{n+1/2}]$, where we recall the definitions of F_n^θ and $F_n^{x_i}$ from Sec. 3.1 and we initialise at $(\mathbf{V}_{n\eta}^\theta, \mathbf{V}_{n\eta}^{x_i}) = (V_{n+\frac{1}{2}}^\theta, V_{n+\frac{1}{2}}^{x_i})$. This results in the update,

$$\begin{aligned} V_{n+\frac{1}{2}}^\theta &= V_{n+\frac{1}{4}}^\theta + \frac{\eta}{2} F_n^\theta, \\ V_{n+\frac{1}{2}}^{x_i} &= V_{n+\frac{1}{4}}^{x_i} + \frac{\eta}{2} \nabla_x F_n^{x_i}. \end{aligned} \tag{B}$$

Finally, the (A) update considers the partial flow,

$$\begin{aligned} d\theta_t &= \mathbf{V}_t^\theta dt, \\ d\mathbf{X}_t^i &= \mathbf{V}_t^{x_i} dt, \end{aligned}$$

over $t \in [t_n, t_{n+1}]$, where we consider $(\mathbf{V}_t^\theta, \mathbf{V}_t^{x_i})$ is frozen at $(V_{n+1/2}^\theta, V_{n+1/2}^{x_i})$ and we initialise at $(\theta_{n\eta}, \mathbf{X}_{n\eta}^i) = (\theta_n, X_n^i)$. Hence, the (A) update is given as,

$$\begin{aligned} \theta_{n+1} &= \theta_n + \eta V_{n+\frac{1}{2}}^\theta, \\ X_{n+1}^i &= X_n^i + \eta V_{n+\frac{1}{2}}^{x_i}. \end{aligned} \tag{A}$$

The algorithm is then completed by repeating steps (B) and (O),

$$\begin{aligned} V_{n+1}^\theta &= \delta \left(V_{n+\frac{1}{2}}^\theta - \frac{\eta}{2} F_{n+1}^\theta \right) + \sqrt{\frac{1 - \delta^2}{N}} \xi_n^{0,\prime}, \\ V_{n+1}^{x_i} &= \delta \left(V_{n+\frac{1}{2}}^{x_i} - \frac{\eta}{2} F_{n+1}^{x_i} \right) + \sqrt{1 - \delta^2} \xi_n^{i,\prime}, \end{aligned} \tag{B+O}$$

over the interval $t \in [t_{n+1/2}, t_{n+1}]$ for standard Gaussians $\xi_n^{0,\prime}$ and $\xi_n^{i,\prime}$ in \mathbb{R}^{d_θ} and \mathbb{R}^{d_x} respectively.

The full updates are given in Algorithm 2 and a full derivation of the KIPLMC2 algorithm is given in Appendix B.

4 Nonasymptotic Analysis

In this section, we provide the convergence results for both the analytic and numerical schemes in the nonasymptotic regime. In Section 4.1, we lay out our assumptions about our target measure. In Section 4.2, we introduce the proof strategy for the reader’s convenience, which may be useful for extending and proving similar results. In Section 4.3, we provide the full nonasymptotic bounds – in particular, in Section 4.3.1, we identify the stationary measure for KIPLD and show an exponential convergence rate to it, as well as, its concentration onto the MMLE solution $\bar{\theta}_*$ as N grows. Following this, in Section 4.3.2, the error bounds for the two algorithms are provided, allowing us to identify the convergence rate of KIPLMC1 and KIPLMC2 to the MMLE solution $\bar{\theta}_*$.

4.1 Assumptions

Our assumptions are generic for the analysis of Langevin diffusions, i.e., we assume strong convexity and L -Lipschitz gradients for the potential U . These assumptions are akin to the assumptions made in Durmus and Moulines [24], Dalalyan [18], Dalalyan and Karagulyan [19] for proving the convergence of ULA. It is, however, possible to relax them, as can be seen in Zhang et al. [53], Akyildiz and Sabanis [1].

We start with the following assumption on the potential U .

H1. *Suppose $U \in C^2$. Let $z, z' \in \mathbb{R}^{d_\theta+d_x}$, we suppose that there exists a μ s.t.*

$$\langle z - z', \nabla U(z) - \nabla U(z') \rangle \geq \mu \|z - z'\|^2.$$

From this follows that $\nabla^2 U$ is positive definite, i.e., $\nabla^2 U(z) \succeq \mu I$ for all $z \in \mathbb{R}^{d_\theta+d_x}$.

This assumption is equivalent to an assumption of joint strong convexity in θ and x for U , which ensures exponentially fast convergence of the KIPLD to the global minimiser and places a quadratic lower growth bound on U . This assumption also means that we can apply the Leibniz differentiation rule under integration for the marginal of the probability model $p_\theta(x, y) = e^{-U(\theta, x)}$ [8, Theorem 16.8]. Next, we provide a smoothness assumption on the potential U .

H2. *We suppose for any $z, z' \in \mathbb{R}^{d_\theta+d_x}$ there exists a constant $L > 0$ s.t.*

$$\|\nabla U(z) - \nabla U(z')\| \leq L \|z - z'\|.$$

This assumption is a common assumption in the analysis of stochastic differential equations, as it ensures stability of the diffusion KIPLD, leading to strong solutions, and stable numerical discretisations [34]. Observe that this assumption places an upper quadratic growth bound on U or, from the perspective of the probabilistic model, $\log p_\theta(x, y)$ is of quadratic growth in both θ and x .

We remark nonetheless that, in the works cited above, the assumptions are on the strong log-concavity of the target measure. In our setting, this corresponds to imposing a structure on the joint statistical model $p_\theta(x, y)$ in θ and x , as our potential is given as $U(\theta, x) = -\log p_\theta(x, y)$. This requires some care on the user side as a statistical model with strongly log-concave posterior $p_\theta(x|y)$ (with fixed θ) may not necessarily satisfy strong log-concavity of $p_\theta(x, y)$ in (x, θ) jointly. We verify in the experimental section that for some generic models such as Bayesian logistic regression, this is possible. As noted above, however, these strong assumptions on the statistical model should not be difficult to relax using the standard non-log-concave sampling results – but this direction is out of scope of the present work which considers the strongly convex case.

4.2 The proof strategy

Let $(\theta_n)_{n \geq 0}$ be the sequence of iterates generated by a numerical scheme, for example, KIPLMC1 or KIPLMC2. Let π_Θ denote the θ -marginal of the stationary measure of the diffusion KIPLD, and $\delta_{\bar{\theta}_*}$ denote the Dirac measure at $\bar{\theta}_*$. Finally, we denote the law of θ_n by $\mathcal{L}(\theta_n)$.

In order to proceed, we first note that the optimisation error is given as $\mathbb{E}[\|\theta_n - \bar{\theta}_*\|^2]^{1/2} = W_2(\mathcal{L}(\theta_n), \delta_{\bar{\theta}_*})$. This is due to the fact that the set of couplings between a measure ν and another measure δ_y contains a single element $\delta_y \otimes \nu$ [45, Section 1.4], thus the infimum in Wasserstein-2 distance is attained by the coupling $\delta_{\bar{\theta}_*} \otimes \mathcal{L}(\theta_n)$. This implies that $\mathbb{E}[\|\theta_n - \bar{\theta}_*\|^2]^{1/2} = W_2(\mathcal{L}(\theta_n), \delta_{\bar{\theta}_*})$ and consequently using triangle inequality

$$\mathbb{E}[\|\theta_n - \bar{\theta}_*\|^2]^{1/2} \leq \underbrace{W_2(\mathcal{L}(\theta_n), \pi_\Theta)}_{\text{convergence}} + \underbrace{W_2(\pi_\Theta, \delta_{\bar{\theta}_*})}_{\text{concentration}}, \quad (8)$$

as the Wasserstein distance is a metric. The first term is the convergence of the numerical scheme to the stationary measure π_Θ which will be proved for each scheme separately. The second term in the right-hand side of (8) is the concentration of the stationary measure π_Θ onto the MMLE solution $\bar{\theta}_*$, which is given by Proposition 2 below.

4.3 Convergence bounds

As outlined above in (8), we will first show the concentration of the stationary measure π_Θ onto the MMLE solution $\bar{\theta}_*$, then show the convergence of the KIPLD to the stationary measure π_Θ . Finally, we will provide the error bounds for the numerical schemes.

4.3.1 Concentration of the stationary measure

This is a non-standard underdamped Langevin diffusion, thus, we need to first identify the stationary measure of the system. Recall that we are only interested in θ -marginal of this stationary measure and we denote it by π_Θ . We first have the following proposition.

Proposition 1. *Let π_Θ be the θ -marginal of the stationary measure of the KIPLD. Then, we can write its density as*

$$\pi_\Theta(\theta) \propto \exp(-N\kappa(\theta)). \quad (9)$$

where $\kappa(\theta) = -\log p_\theta(y)$.

Proof. See Appendix C.1. \square

This result shows that the KIPLD targets the right object: as N grows, π_Θ will concentrate on the minimisers of $\kappa(\theta)$ by a classical result [31]. This shows that the number of particles N acts as an inverse temperature parameter in the underdamped diffusion. Since the minimiser of $\kappa(\theta)$ is the maximiser of $\log p_\theta(y)$, we can see that the stationary measure of the KIPLD is concentrating on the MMLE solution $\bar{\theta}_*$. In particular, under the assumption H1, we have the following nonasymptotic concentration result.

Proposition 2. *Under H1, the function $\theta \mapsto p_\theta(y)$ is μ -strongly log-concave. Furthermore, we have*

$$W_2(\pi_\Theta, \delta_{\bar{\theta}_*}) \leq \sqrt{\frac{d_\theta}{\mu N}},$$

where $\bar{\theta}_* = \operatorname{argmax}_{\theta \in \Theta} \log p_\theta(y)$, which is unique.

Proof. See Appendix C.2. \square

We note here that this result is optimal, as it is achieved when π_Θ is Gaussian and $N\mu$ is the tight lower bound on the eigenvalues of the covariance matrix. We note that such results are also potentially possible under non-convex settings [53, 1].

4.3.2 Convergence of the KIPLD to the stationary measure

We next demonstrate that the KIPLD converges to its stationary measure π_Θ exponentially fast in the strongly log-concave case.

Proposition 3. *Let $(\theta_t)_{t \geq 0}$ be the θ -marginal of a solution to the KIPLD, initialised at $\mathbf{Z}_0 \sim \nu \otimes \mathcal{N}(0, \mathbb{I}_{d_z})$. Then under [H1](#) and [H2](#) and for $\gamma \geq \sqrt{\mu + L}$, we have*

$$W_2(\mathcal{L}(\theta_t), \pi_\Theta) \leq \sqrt{2} \exp\left(-\frac{\mu}{\gamma} t\right) \mathbb{E}[\|\mathbf{Z}_0 - \bar{Z}_\star\|^2]^{1/2},$$

where $\bar{Z}_\star \sim \tilde{\pi}$ is the extended target measure described in [Lemma A.1](#).

Proof. See [Appendix C.3](#). \square

4.3.3 Nonasymptotic analysis of KIPLMC1

In this section we present our first main result, the convergence rate of KIPLMC1.

Theorem 1. *Let $(\theta_n)_{n \in \mathbb{N}}$ be the iterates of KIPLMC1 and suppose that the process is initialised as $(Z_0, V_0^z)^T \sim \nu \otimes \mathcal{N}(0, \mathbb{I}_{d_z})$, where $\nu \in \mathcal{P}(\mathbb{R}^{d_z})$ has bounded second moments. Under [Assumptions H1](#) and [H2](#) and with $\gamma \geq \sqrt{\mu + L}$ and $\eta \leq \mu/(4\gamma L)$, we have*

$$\mathbb{E}[\|\theta_n - \bar{\theta}_\star\|^2]^{1/2} \leq C_1 \left(1 - \frac{0.75\mu\eta}{\gamma}\right)^n + \eta C_2 + \sqrt{\frac{C_3}{N}},$$

where

$$C_1 = \sqrt{2} \mathbb{E}[\|Z_0 - \bar{Z}_\star\|^2]^{1/2}, \quad C_2 = \sqrt{2} \frac{L}{\mu} \sqrt{\frac{d_\theta + Nd_x}{N}}, \quad C_3 = \frac{d_\theta}{\mu},$$

where $Z_0 = (\theta_0, N^{-1/2}X_0^1, \dots, N^{-1/2}X_0^N)^\top$, the initialisation step of the KIPLMC1 where $\bar{Z}_\star \sim \tilde{\pi}$ and $\tilde{\pi}$ is the extended target measure described in [Lemma A.1](#).

Proof. See [Appendix C.4](#). \square

To provide the algorithmic complexity of KIPLMC1, we can inspect the bound provided in [Theorem 1](#). To obtain a complexity result, we first set $N = \mathcal{O}(d_\theta \varepsilon^{-2})$ which ensures the last term in the bound in [Theorem 1](#) is $\mathcal{O}(\varepsilon)$. Next, set $\eta = \mathcal{O}(\varepsilon d_x^{-1/2})$ which ensures that the second term is $\mathcal{O}(\varepsilon)$. It is then easy to see that $n = \tilde{\mathcal{O}}(\varepsilon^{-1} d_x^{1/2})$ steps are enough to obtain $\mathbb{E}[\|\theta_n - \bar{\theta}_\star\|^2]^{1/2} \leq \varepsilon$.

Remark 1. *This dependency needs to be compared with IPLA and PGD. For the former, we note that our dependence to dimension for N is identical to IPLA and the dependence of the number of steps is significantly improved, i.e., we require $n = \tilde{\mathcal{O}}(d_x^{1/2} \varepsilon^{-1})$ whereas IPLA requires $n = \tilde{\mathcal{O}}(d_x \varepsilon^{-2})$ steps for the same accuracy. Regarding the latter method, PGD, our dependence to number of particles is different, as PGD requires $N = \mathcal{O}(d_x \varepsilon^{-2})$ (but this difference is a more general difference stemming from the different analysis techniques, as IPLA also has the same dependence as us to the number of particles N , see, e.g., [Corollary 8](#) and the subsequent discussion in [Caprio et al. \[12\]](#)). However, in terms of the number of steps necessary to attain ε -error, we have the same improvement in dimension dependence in d_x and ε as we have compared to IPLA.*

4.3.4 Nonasymptotic analysis of KIPLMC2

We present our second main result, showing the convergence rate of KIPLMC2.

	step count (n)	N	η
KIPLMC1	$\tilde{\mathcal{O}}(\sqrt{d_x}/\varepsilon)$	$\mathcal{O}(d_\theta/\varepsilon^2)$	$\mathcal{O}(\varepsilon/\sqrt{d_x})$
KIPLMC2	$\tilde{\mathcal{O}}(\sqrt{d_x d_\theta}/\varepsilon^2)$	$\mathcal{O}(d_\theta/\varepsilon^2)$	$\mathcal{O}(\varepsilon^2/\sqrt{d_x d_\theta})$
IPLA	$\tilde{\mathcal{O}}(d_x/\varepsilon^2)$	$\mathcal{O}(d_\theta/\varepsilon^2)$	$\mathcal{O}(\varepsilon^2/d_x)$
PGD	$\tilde{\mathcal{O}}(d_x/\varepsilon^2)$	$\mathcal{O}(d_x/\varepsilon^2)$	$\mathcal{O}(\varepsilon^2/d_x)$

Table 1: Comparison of orders required to achieve an error of order ε in W_2 , for step count, particle number N and step size η .

Theorem 2. Let $(\theta_n)_{n \in \mathbb{N}}$ be the iterates of KIPLMC2 and suppose that the process is initialised as $(Z_0, V_0^z)^T \sim \nu \otimes \mathcal{N}(0, \mathbb{I}_{d_z})$, where $\nu \in \mathcal{P}(\mathbb{R}^{d_z})$ has bounded second moments. Under Assumptions H1 and H2 and with $\gamma \geq 2\sqrt{L}$ and $\eta \leq \frac{\mu}{33\gamma^3}$, we have

$$\mathbb{E}[\|\theta_n - \bar{\theta}_*\|^2]^{1/2} \leq \tilde{C}_1 \left(1 - \frac{\eta\mu}{3\gamma}\right)^{n/2} + \tilde{C}_2\eta + \sqrt{\frac{\tilde{C}_3}{N}},$$

where $Z_0 = (\theta_0, N^{-1/2}X_0^1, \dots, N^{-1/2}X_0^N)^\top$, the initialisation step of the KIPLMC2, $\bar{Z}_* \sim \tilde{\pi}$ and $\tilde{\pi}$ is the extended target measure described in Lemma A.1. The constants $\tilde{C}_1, \tilde{C}_2, \tilde{C}_3$ are given as

$$\tilde{C}_1 = \sqrt{3}(\sqrt{L} \vee \sqrt{L}^{-1})\mathbb{E}[\|Z_0 - \bar{Z}^*\|^2]^{1/2}, \quad \tilde{C}_2 = \sqrt{2(Nd_x + d_\theta)}\frac{6\gamma K}{\mu}\sqrt{3}(\sqrt{L} \vee \sqrt{L}^{-1}), \quad \tilde{C}_3 = \frac{d_\theta}{\mu},$$

where

$$K = L \left(1 + e^{L\eta^2} \left(\frac{\eta}{6} + \frac{\eta^2 L}{24}\right)\right) \left(1 + \frac{\eta L}{2\sqrt{\mu}}\right).$$

Note K converges to L as $\eta \rightarrow 0$.

Proof. See Appendix C.5. \square

To obtain complexity, similarly to the analysis provided for KIPLMC1, we first set $N = \mathcal{O}(\varepsilon^{-2}d_\theta)$ to obtain $\mathcal{O}(\varepsilon)$ dependence in the last term of the bound in Theorem 2, and $\eta = \mathcal{O}(\varepsilon^2(d_x d_\theta)^{-1/2})$ to obtain the same dependence in the second term of the bound in Theorem 2. Finally, setting $n = \tilde{\mathcal{O}}((d_x d_\theta)^{1/2}\varepsilon^{-2})$ brings us an accuracy of ε .

A few comments are in order for this complexity analysis for KIPLMC2.

Remark 2. In general, to avoid poor dependence on N , the error bounds of numerical discretisations must depend on L and μ with the same order. This ensures that the factors cancel out appropriately, preventing any undesirable effects. This is achieved by the analysis of the exponential integrator in Dalalyan and Riou-Durand [20] with a linear dependence on the condition number L/μ , thus our KIPLMC1 bound does not have a bad dependence to N . This enables us to obtain improved algorithmic complexity as discussed in Remark 1. However, for KIPLMC2, the OBABO scheme does not have this dependence on the condition number (see, e.g., Monmarché [41, Table 2]) under just H1 and H2. This results in a bound in Theorem 2 that grows as N grows. This is reflected therefore in the algorithmic complexity as KIPLMC2 theoretically requires $n = \tilde{\mathcal{O}}(\sqrt{d_x d_\theta}\varepsilon^{-2})$ steps to achieve ε error, compared to IPLA which requires $\tilde{\mathcal{O}}(d_x\varepsilon^{-2})$ steps. In this setting, the improvement (in dimension) only happens in the case where $d_\theta \leq d_x$, i.e., the dimension of parameter of the statistical model is less than the dimension of the latent variables.

See Table 1 for a summary of our discussion.

5 Experiments

In the following section a comparison will be made between the empirical results of KIPLMC1, KIPLMC2 algorithms, as well as, those of PGD from Kuntz et al. [35], IPLA from Akyildiz et al. [3] and MPGD from Lim et al. [37]. We note that, in Lim et al. [37], the MPGD is not solely the discretisation of the KIPLD-like SDE using the exponential integrator, but includes a *gradient correction* term, making theoretical analysis and a direct comparison with our methods non-trivial (for a comparison of computational cost see Sec. D.2). To this end, we will also compare these methods to MPGDnc, the MPGD algorithm implemented without gradient correction, so that the number of gradient computations is the same as KIPLMC1.

In the following sections, we will consider three examples: (i) Bayesian logistic regression on a synthetic dataset, (ii) Bayesian logistic regression on the Wisconsin Cancer dataset, and (iii) a Bayesian Neural Network (BNN) example as a more challenging, non-convex example on the MNIST dataset.

5.1 Bayesian Logistic Regression on Synthetic Data

We follow the experimental setting in Kuntz et al. [35] and Akyildiz et al. [3] and start with comparisons between algorithms on a synthetic dataset for which we know the true solution. More precisely, consider the Bayesian logistic regression model

$$p_\theta(x) = \mathcal{N}(x; \theta, \sigma^2 I_{d_x}), \quad p(y|x) = \prod_{j=1}^{d_y} s(v_j^\top x)^{y_j} (1 - s(v_j^\top x))^{1-y_j}.$$

Here $s(u) = e^u / (1 + e^u)$ is the logistic function and v_j , $j \in [d_y]$ are the set of d_x -dimensional covariates with corresponding responses $y_j \in \{0, 1\}$. σ is given and fixed throughout. We generate a synthetic set of covariates, $\{v_j\}_{j=1}^{d_y} \subset \mathbb{R}^{d_x}$, from which are simulated a synthetic set of observations $y_j | \bar{\theta}_*, x, v_j$, for fixed $\bar{\theta}_*$, via a Bernoulli random variable with probability $s(v_j^\top x)$. The algorithm is tested on the recovery of this value of $\bar{\theta}_*$.

The marginal likelihood is given as,

$$p_\theta(y) = \int \left(\prod_{j=1}^{d_y} s(v_j^\top x)^{y_j} (1 - s(v_j^\top x))^{1-y_j} \right) p_\theta(x) dx.$$

From this it easy to see that the gradients of U are given as,

$$\nabla_\theta U(\theta, x) = -\frac{x - \theta}{\sigma^2}, \quad \nabla_x U(\theta, x) = \frac{x - \theta}{\sigma^2} - \sum_{j=1}^{d_y} (y_j - s(v_j^\top x)) v_j. \quad (10)$$

Remark 3 (On H1 and H2). *We will discuss this problem and our assumptions. From (10) it is quite straightforward to observe that,*

$$\begin{aligned} \|\nabla U(z) - \nabla U(z')\| &\leq \frac{2}{\sigma^2} (\|x - x'\| + \|\theta - \theta'\|) + \sum_{j=1}^{d_y} |s(v_j^\top x) - s(v_j^\top x')| \|v_j\| \\ &\leq \left(\frac{2}{\sigma^2} + \frac{1}{4} \sum_{j=1}^{d_y} \|v_j\|^2 \right) \|z - z'\|. \end{aligned}$$

This follows from the fact that the logistic function is Lipschitz continuous with constant 1/4 Akyildiz et al. [3]. Hence, H2 is satisfied.

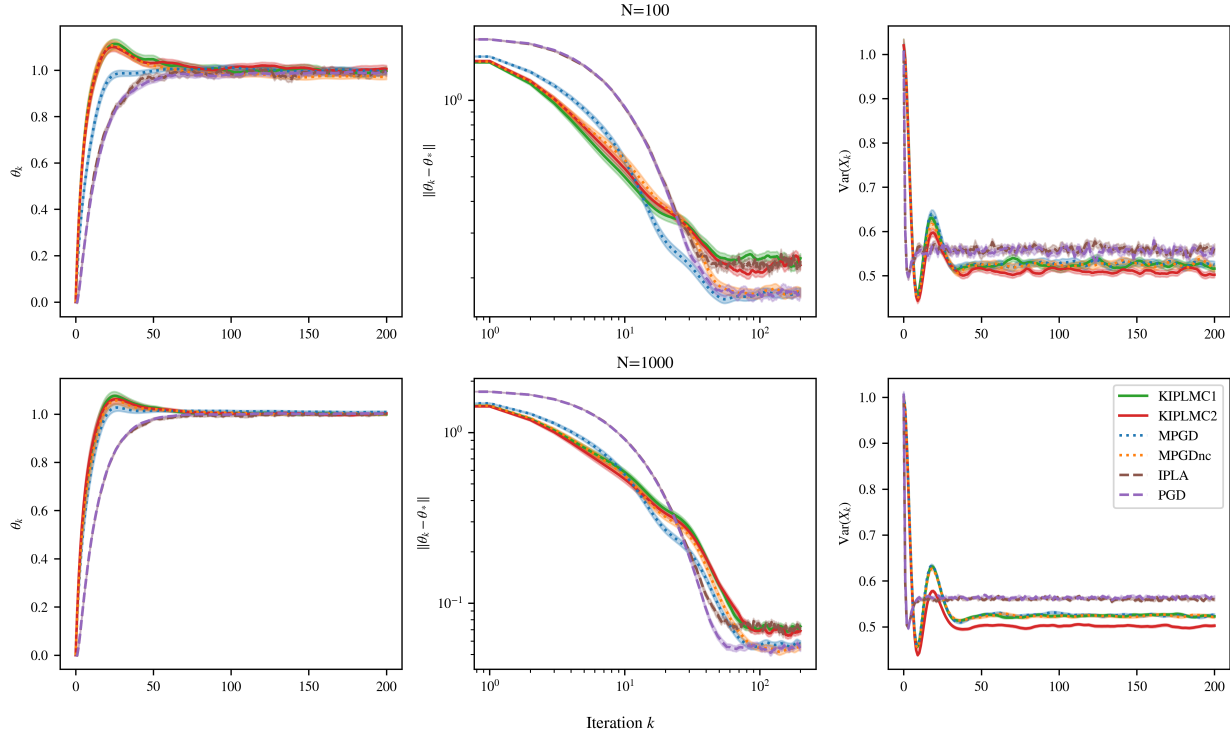


Figure 1: **Parameter estimate comparison.** We compare the performance of the PGD, IPLA, MPGD, KIPLMC1, and KIPLMC2 algorithms on the synthetic dataset with true $\bar{\theta}_* = \mathbb{1}_{d_x}$. We observe the desired convergence of behaviours for larger values of N in the parameter space, mean-square error and the posterior variance of X_k^i . In this example $d_x = d_\theta = 3$, $d_y = 100$ and $\gamma = 2.2$. Here we choose $\theta_0, X_0^i, V_0^\theta, V_0^{x^i} \sim \mathcal{N}(0, 0.1)$ and run 100 Monte Carlo simulations.

For *H1*, consider

$$\nabla^2 U(z) = \frac{1}{\sigma^2} \begin{pmatrix} I_{d_\theta} & -I_{d_x} \\ -I_{d_x} & I_{d_\theta} \end{pmatrix} + \sum_{j=1}^{d_y} s(v_j^\top x)(1 - s(v_j^\top x))v_j \otimes v_j.$$

The sum is positive definite and the matrix was shown by Kuntz et al. [35] to have $2d_\theta$ positive eigenvalues and so it follows that $\nabla^2 U$ is positive definite. Hence U is strictly convex and in theory no lower bound for strong convexity constant exists. We show however this is not a problem for our practical implementations.

In Fig. 1 we can see the difference in the behaviours between the algorithms. Most notably, the KIPLMC1 and KIPLMC2 algorithms exhibit comparable levels of acceleration as the MPGD algorithm in the θ -dimension, whilst the IPLA and PGD algorithms trail further behind. Interestingly, we observe (more notably for large N) that the noise in the θ -dynamics in KIPLMC1 and KIPLMC2, as compared to MPGD, seems to dampen some of the momentum effects when γ , the friction coefficient is sub-optimal. As N grows the θ iterates concentrate onto the MMLE $\bar{\theta}_*$ for all algorithms. This behaviour can be seen in more detail in Fig. 2 (b), in which we can verify the variance changing with rate $\mathcal{O}(1/N)$. Further, we make a comparison of the performance of the IPLA and KIPLMC2 in Fig. 2 (a) with the Area Below the Curve (ABC) metric (see D.3 for more detail). This metric is a signed, weighted difference between the performances of the two algorithms: the higher the value, the better KIPLMC2 performs compared to IPLA; 0 is when they perform the same. We observe that the acceleration of KIPLMC2 can be best observed in specific γ regimes, which ensure that the momentum is close to critical dampening.

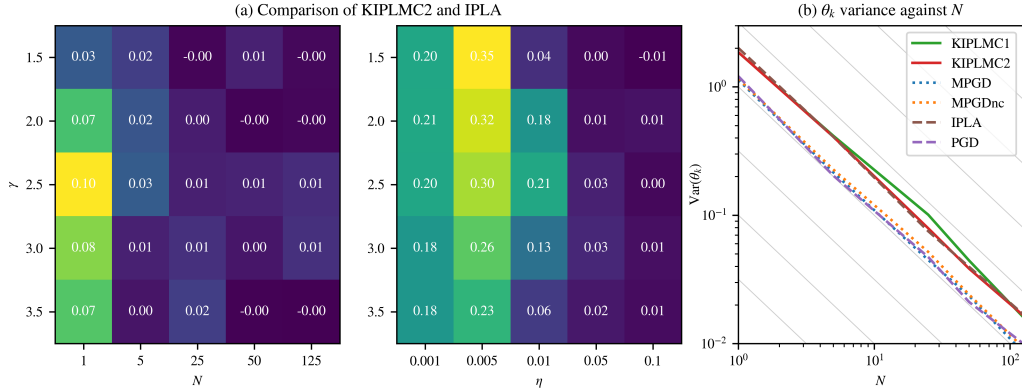


Figure 2: **Comparison over hyper-parameters.** (a) shows the Area Between the Curve (ABC) values between IPLA and KIPLMC2 for a variety of hyper-parameter combinations. The larger the positive value, the greater the acceleration of KIPLMC2 with respect to IPLA (discussed in C.1). (b) makes a comparison over 100 Monte Carlo simulations of the algorithms’ sample variances, using the last 100 steps of each simulation. The grid-lines corresponding to $1/N$ are provided to highlight the rate of convergence. Where not specified otherwise, simulations are run with $M = 2000$, $\eta = 0.005$, $\gamma = 2.2$ and $N = 100$.

Note that the momentum effects of the KIPLMC1 and KIPLMC2 algorithms has been dampened through a specific choice of γ . In training it was observed that the convergence rate is very sensitive to the choice of γ , where choices too small, exhibit large momentum effects, and too large, lead to slow convergence (see also Lim et al. [37] for more discussion on the role of the momentum parameter for learning with KLMC). The choice of γ here is far from optimal, but allows us to observe the strength of the proposed algorithms.

5.2 Wisconsin Cancer Data

We follow again an experimental procedure that is similar to the one outlined in Kuntz et al. [35] and Akyildiz et al. [3] and make comparisons between the algorithms on a more realistic dataset: the Wisconsin Cancer Data. Again, we use the logistic regression LVM model, outlined above. This task is a binary classification, to determine from 9 features gathered from tumors and 693 data points labelled as either benign or malignant. The latent variables correspond to the features extracted from the data. The task in this case is to seek to model the behaviour as accurately as possible through the logistic regression LVM.

For this setup we define our probability model as,

$$p_{\theta}(x) = \mathcal{N}(x; \theta \mathbb{1}_{d_x}, 5I_{d_x})$$

and the likelihood as,

$$p(y|x) = \prod_{j=1}^{d_y} s(v_j^T x)^{y_j} (1 - s(v_j^T x))^{1-y_j}.$$

Note that the parameter θ is a scalar in this case, hence, this turns out to be a simplified version of the setup described above and so the discussion in Remark 3 is still valid. As opposed to the previous case with synthetic data, here we consider a real dataset, thus we do not have access to the true dataset. Hence, there is no comparison to a $\bar{\theta}_*$, but we can see that different algorithms attain similar values as the estimate of this minimum.

Most notably in this experiment, we can observe in Fig. 3 the importance of the added stability that the momentum-based algorithms exhibit, with the use of more stable numerical integrators than Euler-Maruyama. In particular, these algorithms displays great stability w.r.t. the choice of the step-size, as well as, the acceleration one would expect. For small step-sizes, the PGD algorithm performs with low variance in all

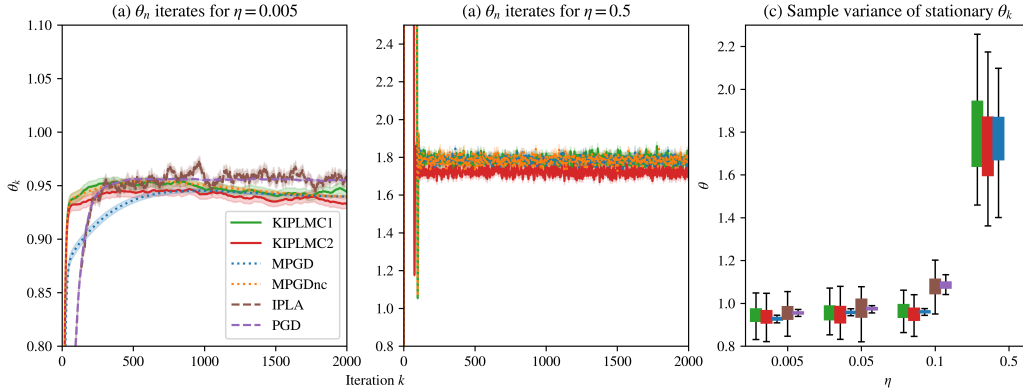


Figure 3: **Wisconsin Dataset.** The performance of PGD, IPLA, MPGD, KIPLMC1 and KIPLMC2 algorithms are compared on a logistic regression experiment for the Wisconsin Cancer Dataset. In (a), we show the behaviour of the θ_n iterates for a small step-size and (b) shows the behaviour θ_n iterates for a step-size where IPLA and PGD explode. In (c) we compare the distributions of the algorithms over different step-sizes. We set $N = 100$ and $\gamma = 3.2$.

cases where it converges, until it explodes where step-sizes become too large. It is interesting to note however that in the large step-size regime, the momentum-based algorithms exhibit much greater momentum than in the smaller step-sizes. However, again, we note that the KIPLMC1 and KIPLMC2 algorithms exhibit more variance in the θ estimation than the PGD and MPGD algorithms, though it is damped when compared to the IPLA algorithm, due to the higher regularity of the solutions to KIPLD. This is typically an advantage when working with convex problems, but this “sticky” behaviour might prove detrimental in the non-convex case [27, 3]. The injection of noise into the parameter estimation may help the method to escape local minima [1].

5.3 Bayesian Neural Network

Similarly to Kuntz et al. [35], Lim et al. [37] we also consider a Bayesian Neural Network (BNN) example to perform character classification on the MNIST dataset. In this case our approach is similar to “cold” posterior estimation, as our sampling density is proportional to a density raised to the inverse temperature, as in Wenzel et al. [51].

This dataset and model provide a more challenging problem for the KIPLMC1 and KIPLMC2 algorithms as the posteriors are known to be multi-modal and hence do not satisfy assumption H1. MNIST contains 70’000 28×28 grey-scale images $\{f_i\}_{i=1}^{70000} \subset \mathbb{R}^{784}$. However, to avoid issues of high dimensionality, we consider a normalised subset of 1,000 characters containing only images of fours and nines, whose similarity should pose a challenge. Due to this smaller sample, we are also able to avoid the need for sub-sampling.

Following Kuntz et al. [35] we employ a two layer BNN with tanh activation function, softmax output layer and 40 dimensional latent space. i.e. we consider the probability of the data labels l to be conditionally independent, given the features f and the weights $x = (w, v)$, with model,

$$p(l|f, x) \propto \exp \left(\sum_{j=1}^{40} v_{lj} \tanh \left(\sum_{i=1}^{784} w_{ji} f_i \right) \right),$$

where $w \in \mathbb{R}^{40 \times 784}$, $v \in \mathbb{R}^{2 \times 40}$. Consider the priors on the weights to be without bias and Gaussian: $w \sim \mathcal{N}(0, e^{2\alpha} \mathbb{I})$ and $v \sim \mathcal{N}(0, e^{2\beta} \mathbb{I})$. Rather than assigning these priors, we learn the parameters $\theta = (\alpha, \beta) \in \mathbb{R}^2$

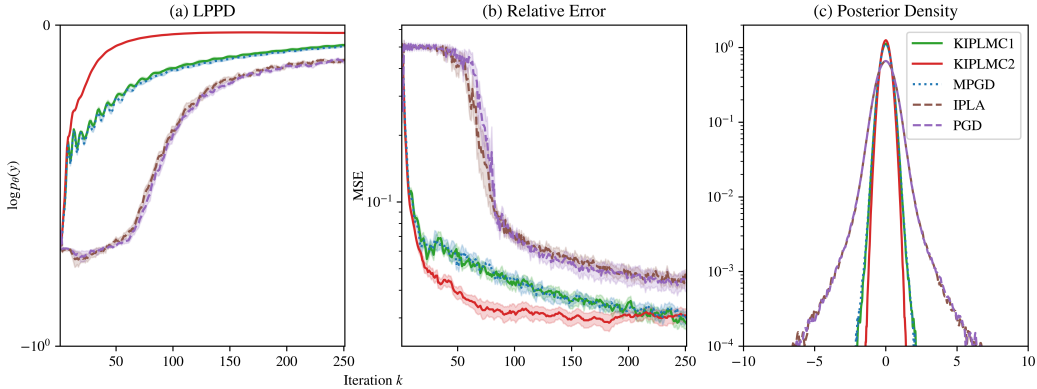


Figure 4: **MNIST Dataset.** The performance of PGD, IPLA, MPGD, KIPLMC1 and KIPLMC2 algorithms are compared on a classification experiment for the MNIST Dataset. (a) shows the Log Pointwise Predictive Density, the average log probability assigned to the correct response. (b) shows the percentage error and (c) the posterior density of the weights w . For this experiment $N = 100$, $\gamma = 2$ and $\eta = 0.01$.

jointly with the latent variables x . Hence, the model’s density is given as

$$p_{\theta}(x, \{f_i\}_{i=1}^{1000}) = \mathcal{N}(w; 0, e^{2\alpha}) \mathcal{N}(v; 0, e^{2\beta}) \prod_{i=1}^{1000} p(l|f_i, x).$$

We will employ autograd methods from the PyTorch library to compute the gradients.

In Fig. 4 we make a comparison between the different algorithms over 100 runs, comparing the log predictive point-wise density (LPPD) and relative error. The LPPD is the average log-likelihood assigned to the correct response, whilst the relative error is given as the accuracy of prediction on a test set (see D.4 for more detail). Observe the improved behaviour of the momentum-based algorithms in LPPD, as well as relative error. We also note the significant acceleration observed for KIPLMC2, highlighting the effect of the distinct numerical integrators. Similarly, in Fig. 4 (c) we can see the more concentrated posterior distributions of the momentum-based algorithms. Thus it is clear that the KIPLMC1 and KIPLMC2 algorithms perform competitively against other particle-based methods, even in very complex problems, in which our assumptions may not be satisfied.

6 Conclusions

This paper extends a line of work on interacting particle-, and more generally, diffusion-based algorithms for maximum marginal likelihood estimation. This paper has focused on alternatives to the interacting particle systems (IPs) proposed by Kuntz et al. [35], Akyildiz et al. [3], Lim et al. [37] for the MMLE problem by considering an accelerated variant. We have shown that we can leverage the existing literature on underdamped Langevin diffusion for sampling [20, 16, 41, 39] to produce two algorithms with greater stability, added smoothness and exponential convergence, which concentrate onto the MMLE with quantitative nonasymptotic bounds on the estimation error $\mathbb{E}[\|\theta_n - \bar{\theta}_*\|^2]^{1/2}$. In particular, we show that KIPLMC1 attains an accelerated error rate for error ε after $\tilde{\mathcal{O}}(\sqrt{d_x}\varepsilon^{-1})$ steps, compared to the IPLA and PGD which require $\tilde{\mathcal{O}}(d_x\varepsilon^{-2})$ steps. The proposed algorithms both perform well empirically compared to the MPGD (with equal choice of step-sizes and friction coefficients) and other particle methods. Specifically, the induced noise should improve guarantees in the non-convex setting, as discussed in Akyildiz et al. [3], Raginsky et al. [44], Akyildiz and Sabanis [1].

The results presented here hold under assumptions of gradient-Lipschitzness and strong log-concavity, however, it is possible to extend this line of work to the non-convex, super-linear or even proximal cases

(for examples of this see, Zhang et al. [53], Akyildiz and Sabanis [1], Johnston et al. [32], Cordero-Encinar et al. [17]). Another interesting direction is to consider the setting in Fan et al. [26], using an accelerated algorithm for high-dimensional linear models. Our methods can also be adapted to solving linear inverse problems as done by Akyildiz et al. [4], Glyn-Davies et al. [28]. Similar ideas can be considered within the setting of Stein variational gradient descent as done in Sharrock et al. [47]. Crucially, the procedure used to obtain the bounds for the algorithms presented here can easily be extended to other cases, creating a powerful theoretical framework for further underdamped Langevin sampling algorithms for the MMLE problem.

Acknowledgements

We would like to thank Juan Kuntz and Paula Cordero Encinar for their insightful comments and suggestions. PVO is supported by the EPSRC through the Modern Statistics and Statistical Machine Learning (StatML) CDT programme, grant no. EP/S023151/1.

References

- [1] Ö. Deniz Akyildiz and Sotirios Sabanis. Nonasymptotic analysis of stochastic gradient hamiltonian monte carlo under local conditions for nonconvex optimization. *Journal of Machine Learning Research*, 25(113):1–34, 2024. Cited on pages 9, 10, 16, 17, and 18.
- [2] Ö. Deniz Akyildiz, Michela Ottobre, and Iain Souttar. A multiscale perspective on maximum marginal likelihood estimation. *arXiv preprint arXiv:2406.04187*, 2024. Cited on page 2.
- [3] Ö. Deniz Akyildiz, Francesca Romana Crucinio, Mark Girolami, Tim Johnston, and Sotirios Sabanis. Interacting particle Langevin algorithm for maximum marginal likelihood estimation. *ESAIM: Probability and Statistics*, 2025. Cited on pages 2, 3, 4, 13, 15, 16, and 17.
- [4] Ömer Deniz Akyildiz, Connor Duffin, Sotirios Sabanis, and Mark Girolami. Statistical finite elements via Langevin dynamics. *SIAM/ASA Journal on Uncertainty Quantification*, 10(4):1560–1585, 2022. Cited on page 18.
- [5] Jason M. Altschuler and Sinho Chewi. Faster high-accuracy log-concave sampling via algorithmic warm starts. *J. ACM*, 71(3), June 2024. ISSN 0004-5411. doi: 10.1145/3653446. URL <https://doi.org/10.1145/3653446>. Cited on page 29.
- [6] Yves F. Atchadé, Gersende Fort, and Eric Moulines. On perturbed proximal gradient algorithms. *Journal of Machine Learning Research*, 18(10):1–33, 2017. URL <http://jmlr.org/papers/v18/15-038.html>. Cited on pages 2 and 4.
- [7] José M Bernardo and Adrian FM Smith. *Bayesian theory*, volume 405. John Wiley & Sons, New York, 2009. Cited on page 1.
- [8] P. Billingsley. *Probability and Measure*. Wiley Series in Probability and Statistics. Wiley, Hoboken, 1995. ISBN 9780471007104. Cited on page 9.
- [9] David M Blei, Andrew Y Ng, and Michael I Jordan. Latent Dirichlet allocation. *Journal of Machine Learning Research*, 3(Jan):993–1022, 2003. Cited on page 1.
- [10] James G Booth and James P Hobert. Maximizing generalized linear mixed model likelihoods with an automated Monte Carlo EM algorithm. *Journal of the Royal Statistical Society: Series B (Statistical Methodology)*, 61(1):265–285, 1999. Cited on page 2.
- [11] Olivier Cappé, Arnaud Doucet, Marc Lavielle, and Eric Moulines. Simulation-based methods for blind maximum-likelihood filter identification. *Signal Processing*, 73(1-2):3–25, 1999. Cited on page 2.

- [12] Rocco Caprio, Juan Kuntz, Samuel Power, and Adam M Johansen. Error bounds for particle gradient descent, and extensions of the log-sobolev and talagrand inequalities. *Journal of Machine Learning Research*, 26(103):1–38, 2025. Cited on pages 2 and 11.
- [13] Gilles Celeux. The SEM algorithm: a probabilistic teacher algorithm derived from the em algorithm for the mixture problem. *Computational Statistics Quarterly*, 2:73–82, 1985. Cited on page 2.
- [14] Gilles Celeux and Jean Diebolt. A stochastic approximation type EM algorithm for the mixture problem. *Stochastics: An International Journal of Probability and Stochastic Processes*, 41(1-2):119–134, 1992. Cited on page 2.
- [15] KS Chan and Johannes Ledolter. Monte Carlo EM estimation for time series models involving counts. *Journal of the American Statistical Association*, 90(429):242–252, 1995. Cited on page 2.
- [16] Xiang Cheng, Niladri S Chatterji, Peter L Bartlett, and Michael I Jordan. Underdamped Langevin MCMC: A non-asymptotic analysis. In *Conference On Learning Theory*, pages 300–323, 2018. Cited on pages 4 and 17.
- [17] Paula Cordero-Encinar, Francesca R Crucinio, and O Deniz Akyildiz. Proximal interacting particle Langevin algorithms. *Uncertainty in Artificial Intelligence (UAI)*, 2025. Cited on pages 2 and 18.
- [18] Arnak S Dalalyan. Theoretical guarantees for approximate sampling from smooth and log-concave densities. *Journal of the Royal Statistical Society: Series B (Statistical Methodology)*, 79(3):651–676, 2017. Cited on pages 2, 3, 4, and 9.
- [19] Arnak S Dalalyan and Avetik Karagulyan. User-friendly guarantees for the Langevin Monte Carlo with inaccurate gradient. *Stochastic Processes and their Applications*, 129(12):5278–5311, 2019. Cited on page 9.
- [20] Arnak S Dalalyan and Lionel Riou-Durand. On sampling from a log-concave density using kinetic langevin diffusions. *Bernoulli*, 26(3):1956–1988, 2020. Cited on pages 4, 5, 12, 17, 25, 29, and 30.
- [21] Valentin De Bortoli, Alain Durmus, Marcelo Pereyra, and Ana F Vidal. Efficient stochastic optimisation by unadjusted langevin monte carlo. *Statistics and Computing*, 31(3):1–18, 2021. Cited on pages 2 and 4.
- [22] Arthur P Dempster, Nan M Laird, and Donald B Rubin. Maximum likelihood from incomplete data via the em algorithm. *Journal of the Royal Statistical Society: Series B (Methodological)*, 39(1):1–22, 1977. Cited on page 1.
- [23] J Diebolt and E HS Ip. A stochastic EM algorithm for approximating the maximum likelihood estimate. In W. R. Gilks, S. T. Richardson, and D. J. Spiegelhalter, editors, *Markov Chain Monte Carlo in Practice*. CRC Publishers, Boca Raton, 1996. Cited on page 2.
- [24] Alain Durmus and Eric Moulines. Nonasymptotic convergence analysis for the unadjusted Langevin algorithm. *The Annals of Applied Probability*, 27(3):1551–1587, 2017. Cited on pages 2 and 9.
- [25] Alain Durmus and Eric Moulines. High-dimensional Bayesian inference via the unadjusted Langevin algorithm. *Bernoulli*, 25(4A):2854–2882, 2019. Cited on pages 2, 3, and 4.
- [26] Zhou Fan, Leying Guan, Yandi Shen, and Yihong Wu. Gradient flows for empirical bayes in high-dimensional linear models. *arXiv preprint arXiv:2312.12708*, 2023. Cited on page 18.
- [27] Xuefeng Gao, Mert Gürbüzbalaban, and Lingjiong Zhu. Global convergence of stochastic gradient hamiltonian monte carlo for nonconvex stochastic optimization: Nonasymptotic performance bounds and momentum-based acceleration. *Operations Research*, 70(5):2931–2947, 2022. Cited on page 16.

- [28] Alex Glyn-Davies, Connor Duffin, Ieva Kazlauskaitė, Mark Girolami, and Ö Deniz Akyildiz. Statistical finite elements via interacting particle Langevin dynamics. *SIAM/ASA Journal on Uncertainty Quantification*, 13(3):1200–1227, 2025. Cited on pages 1 and 18.
- [29] Peter D Hoff, Adrian E Raftery, and Mark S Handcock. Latent space approaches to social network analysis. *Journal of the American Statistical Association*, 97(460):1090–1098, 2002. Cited on page 1.
- [30] Alan M. Horowitz. A generalized guided monte carlo algorithm. *Physics Letters B*, 268(2):247–252, 1991. ISSN 0370-2693. doi: [https://doi.org/10.1016/0370-2693\(91\)90812-5](https://doi.org/10.1016/0370-2693(91)90812-5). URL <https://www.sciencedirect.com/science/article/pii/0370269391908125>. Cited on page 7.
- [31] Chii-Ruey Hwang. Laplace’s method revisited: weak convergence of probability measures. *The Annals of Probability*, pages 1177–1182, 1980. Cited on pages 4 and 10.
- [32] Tim Johnston, Iosif Lytras, and Sotirios Sabanis. Kinetic langevin mcmc sampling without gradient lipschitz continuity-the strongly convex case. *Journal of Complexity*, 2024. Cited on page 18.
- [33] Tim Johnston, Nikolaos Makras, and Sotirios Sabanis. Taming the interacting particle langevin algorithm: The superlinear case. *Applied Mathematics & Optimization*, 91(3):77, 2025. doi: 10.1007/s00245-025-10269-z. URL <https://doi.org/10.1007/s00245-025-10269-z>. Cited on page 2.
- [34] Peter Eris Kloeden, Eckhard Platen, and Henri Schurz. *Numerical solution of SDE through computer experiments*. Universitext. Springer, Berlin, Germany, 1 edition, December 1993. Cited on page 9.
- [35] Juan Kuntz, Jen Ning Lim, and Adam M Johansen. Particle algorithms for maximum likelihood training of latent variable models. In *International Conference on Artificial Intelligence and Statistics*, pages 5134–5180. PMLR, 2023. Cited on pages 2, 4, 13, 14, 15, 16, 17, and 33.
- [36] Kenneth Lange. A gradient algorithm locally equivalent to the em algorithm. *Journal of the Royal Statistical Society: Series B (Methodological)*, 57(2):425–437, 1995. Cited on page 2.
- [37] Jen Ning Lim, Juan Kuntz, Samuel Power, and Adam M Johansen. Momentum particle maximum likelihood. In *Proceedings of 41st International Conference on Machine Learning (ICML)*, volume 235, 2024. Cited on pages 3, 13, 15, 16, 17, 31, and 33.
- [38] Chuanhai Liu and Donald B Rubin. The ecme algorithm: a simple extension of em and ecm with faster monotone convergence. *Biometrika*, 81(4):633–648, 1994. Cited on page 2.
- [39] Yi-An Ma, Niladri S. Chatterji, Xiang Cheng, Nicolas Flammarion, Peter L. Bartlett, and Michael I. Jordan. Is there an analog of Nesterov acceleration for gradient-based MCMC? *Bernoulli*, 27(3):1942 – 1992, 2021. doi: 10.3150/20-BEJ1297. URL <https://doi.org/10.3150/20-BEJ1297>. Cited on page 17.
- [40] Xiao-Li Meng and Donald B Rubin. Maximum likelihood estimation via the ecm algorithm: A general framework. *Biometrika*, 80(2):267–278, 1993. Cited on page 2.
- [41] Pierre Monmarché. High-dimensional MCMC with a standard splitting scheme for the underdamped Langevin diffusion. *Electronic Journal of Statistics*, 15(2):4117–4166, 2021. Cited on pages 5, 7, 8, 12, 17, 27, and 30.
- [42] Bernt Oksendal. *Stochastic differential equations: an introduction with applications*. Springer Science & Business Media, 2013. Cited on page 6.
- [43] Grigorios A. Pavliotis. *Stochastic processes and applications: Diffusion Processes, the Fokker-Planck and langevin equations*. Springer, New York, 2014. Cited on pages 3 and 4.

- [44] Maxim Raginsky, Alexander Rakhlin, and Matus Telgarsky. Non-convex learning via Stochastic Gradient Langevin Dynamics: a nonasymptotic analysis. In *Conference on Learning Theory*, pages 1674–1703, 2017. Cited on page [17](#).
- [45] Filippo Santambrogio. Optimal transport for applied mathematicians. *Birkäuser, NY*, 55(58-63):94, 2015. Cited on page [10](#).
- [46] Adrien Saumard and Jon A Wellner. Log-concavity and strong log-concavity: a review. *Statistics surveys*, 8:45, 2014. Cited on page [29](#).
- [47] Louis Sharrock, Daniel Dodd, and Christopher Nemeth. Tuning-free maximum likelihood training of latent variable models via coin betting. In *International Conference on Artificial Intelligence and Statistics*, pages 1810–1818. PMLR, 2024. Cited on page [18](#).
- [48] Robert P Sherman, Yu-Yun K Ho, and Siddhartha R Dalal. Conditions for convergence of Monte Carlo EM sequences with an application to product diffusion modeling. *The Econometrics Journal*, 2(2): 248–267, 1999. Cited on page [2](#).
- [49] Paris Smaragdīs, Bhiksha Raj, and Madhusudana Shashanka. A probabilistic latent variable model for acoustic modeling. *Advances in Models for Acoustic Processing Workshop, NIPS*, 148:8–1, 2006. Cited on page [1](#).
- [50] Greg CG Wei and Martin A Tanner. A Monte Carlo implementation of the EM algorithm and the poor man’s data augmentation algorithms. *Journal of the American Statistical Association*, 85(411):699–704, 1990. Cited on page [2](#).
- [51] Florian Wenzel, Kevin Roth, Bastiaan Veeling, Jakub Swiatkowski, Linh Tran, Stephan Mandt, Jasper Snoek, Tim Salimans, Rodolphe Jenatton, and Sebastian Nowozin. How good is the Bayes posterior in deep neural networks really? In Hal Daumé and Aarti Singh, editors, *Proceedings of the 37th International Conference on Machine Learning*, volume 119 of *Proceedings of Machine Learning Research*, pages 10248–10259, Online, July 2020. PMLR. Cited on page [16](#).
- [52] Nick Whiteley, Annie Gray, and Patrick Rubin-Delanchy. Statistical exploration of the manifold hypothesis. *Journal of the Royal Statistical Society: Series B*, 2025. Cited on page [1](#).
- [53] Ying Zhang, Ö. Deniz Akyildiz, Theodoros Damoulas, and Sotirios Sabanis. Nonasymptotic estimates for stochastic gradient langevin dynamics under local conditions in nonconvex optimization. *Applied Mathematics & Optimization*, 87(2):25, 2023. Cited on pages [9](#), [10](#), and [18](#).

Appendix

A Preliminary results

In this section, we prove a key result that rewrites the KIPLD as a single underdamped Langevin diffusion evolving in $\mathbb{R}^{d_\theta + Nd_x}$ with a rescaled potential function and friction coefficient. This will be useful in the analysis of the KIPLD and its discretisation, as it allows us to leverage existing results on underdamped Langevin diffusions.

Proposition A.1. *Let*

$$(\boldsymbol{\theta}_t, \mathbf{X}_t^1, \dots, \mathbf{X}_t^N, \mathbf{V}_t^\theta, \mathbf{V}_t^{x_1}, \dots, \mathbf{V}_t^{x_N})_{t \geq 0}$$

solve (KIPLD). Define

$$\begin{aligned} \tilde{\boldsymbol{\theta}}_t &:= \boldsymbol{\theta}_{\sqrt{N}t}, & \tilde{\mathbf{X}}_t^i &:= N^{-1/2} \mathbf{X}_{\sqrt{N}t}^i, \\ \tilde{\mathbf{V}}_t^\theta &:= \sqrt{N} \mathbf{V}_{\sqrt{N}t}^\theta, & \tilde{\mathbf{V}}_t^{x_i} &:= \mathbf{V}_{\sqrt{N}t}^{x_i}, \end{aligned}$$

for $i \in [N]$, and set

$$\tilde{\mathbf{Z}}_t := (\tilde{\boldsymbol{\theta}}_t, \tilde{\mathbf{X}}_t^1, \dots, \tilde{\mathbf{X}}_t^N)^\top \in \mathbb{R}^{d_\theta + Nd_x}, \quad \tilde{\mathbf{V}}_t^z := (\tilde{\mathbf{V}}_t^\theta, \tilde{\mathbf{V}}_t^{x_1}, \dots, \tilde{\mathbf{V}}_t^{x_N})^\top \in \mathbb{R}^{d_\theta + Nd_x},$$

and

$$\bar{U}_N(\theta, x_1, \dots, x_N) := \frac{1}{N} \sum_{i=1}^N U(\theta, \sqrt{N} x_i), \quad (11)$$

and $\tilde{\gamma} := \sqrt{N}\gamma$. Then there exists a $\mathbb{R}^{d_\theta + Nd_x}$ -valued Brownian motion $(\tilde{\mathbf{B}}_t)_{t \geq 0}$ such that

$$\begin{aligned} d\tilde{\mathbf{Z}}_t &= \tilde{\mathbf{V}}_t^z dt, \\ d\tilde{\mathbf{V}}_t^z &= -\tilde{\gamma} \tilde{\mathbf{V}}_t^z dt - N \nabla_z \bar{U}_N(\tilde{\mathbf{Z}}_t) dt + \sqrt{2\tilde{\gamma}} d\tilde{\mathbf{B}}_t. \end{aligned} \quad (12)$$

Proof. By definition of the rescaled variables, we have

$$d\tilde{\boldsymbol{\theta}}_t = \sqrt{N} d\boldsymbol{\theta}_{\sqrt{N}t} = \sqrt{N} \mathbf{V}_{\sqrt{N}t}^\theta dt = \tilde{\mathbf{V}}_t^\theta dt.$$

Fix $i \in [N]$ and set $s(t) := \sqrt{N}t$. From (KIPLD), $d\mathbf{X}_t^i = \mathbf{V}_t^{x_i} dt$, so

$$d\mathbf{X}_{s(t)}^i = \mathbf{V}_{s(t)}^{x_i} ds(t) = \sqrt{N} \mathbf{V}_{\sqrt{N}t}^{x_i} dt.$$

Hence

$$d\tilde{\mathbf{X}}_t^i = N^{-1/2} d\mathbf{X}_{\sqrt{N}t}^i = N^{-1/2} \sqrt{N} \mathbf{V}_{\sqrt{N}t}^{x_i} dt = \tilde{\mathbf{V}}_t^{x_i} dt,$$

and therefore $d\tilde{\mathbf{Z}}_t = \tilde{\mathbf{V}}_t^z dt$. Next, define $\tilde{\mathbf{B}}_t^j := N^{-1/4} \mathbf{B}_{\sqrt{N}t}^j$ for $j = 0, \dots, N$; then each $\tilde{\mathbf{B}}_t^j$ is a Brownian motion and $d\mathbf{B}_{\sqrt{N}t}^j = N^{1/4} d\tilde{\mathbf{B}}_t^j$. Using (KIPLD), set $s(t) := \sqrt{N}t$. Then

$$\begin{aligned} d\tilde{\mathbf{V}}_t^\theta &= \sqrt{N} d\mathbf{V}_{s(t)}^\theta \\ &= \sqrt{N} \left[\left(-\gamma \mathbf{V}_{s(t)}^\theta - \frac{1}{N} \sum_{i=1}^N \nabla_\theta U(\boldsymbol{\theta}_{s(t)}, \mathbf{X}_{s(t)}^i) \right) ds(t) + \sqrt{\frac{2\gamma}{N}} d\mathbf{B}_{s(t)}^0 \right] \\ &= -N\gamma \mathbf{V}_{\sqrt{N}t}^\theta dt - \sum_{i=1}^N \nabla_\theta U(\boldsymbol{\theta}_{\sqrt{N}t}, \mathbf{X}_{\sqrt{N}t}^i) dt + \sqrt{2\gamma\sqrt{N}} d\tilde{\mathbf{B}}_t^0 \\ &= -\tilde{\gamma} \tilde{\mathbf{V}}_t^\theta dt - N \nabla_\theta \bar{U}_N(\tilde{\mathbf{Z}}_t) dt + \sqrt{2\tilde{\gamma}} d\tilde{\mathbf{B}}_t^0, \end{aligned}$$

where we used $ds(t) = \sqrt{N}dt$ and

$$N \nabla_\theta \bar{U}_N(\tilde{\mathbf{Z}}_t) = \sum_{i=1}^N \nabla_\theta U(\boldsymbol{\theta}_{\sqrt{N}t}, \mathbf{X}_{\sqrt{N}t}^i).$$

Fix $i \in [N]$. Using again $s(t) = \sqrt{N}t$ and (KIPLD),

$$\begin{aligned} d\tilde{\mathbf{V}}_t^{x_i} &= d\mathbf{V}_{s(t)}^{x_i} \\ &= \left(-\gamma \mathbf{V}_{s(t)}^{x_i} - \nabla_x U(\boldsymbol{\theta}_{s(t)}, \mathbf{X}_{s(t)}^i) \right) ds(t) + \sqrt{2\gamma} d\mathbf{B}_{s(t)}^i \\ &= -\sqrt{N}\gamma \mathbf{V}_{\sqrt{N}t}^{x_i} dt - \sqrt{N} \nabla_x U(\boldsymbol{\theta}_{\sqrt{N}t}, \mathbf{X}_{\sqrt{N}t}^i) dt + \sqrt{2\gamma\sqrt{N}} d\tilde{\mathbf{B}}_t^i \\ &= -\tilde{\gamma} \tilde{\mathbf{V}}_t^{x_i} dt - N \nabla_{z_i} \bar{U}_N(\tilde{\mathbf{Z}}_t) dt + \sqrt{2\tilde{\gamma}} d\tilde{\mathbf{B}}_t^i, \end{aligned}$$

where

$$N \nabla_{z_i} \bar{U}_N(\tilde{\mathbf{Z}}_t) = \sqrt{N} \nabla_x U(\boldsymbol{\theta}_{\sqrt{N}t}, \mathbf{X}_{\sqrt{N}t}^i).$$

Stacking coordinates and defining $\tilde{\mathbf{B}}_t = (\tilde{\mathbf{B}}_t^0, \tilde{\mathbf{B}}_t^1, \dots, \tilde{\mathbf{B}}_t^N)^\top$ gives (12). \square

Next we show that the stationary measure of the dynamics in (12) is given by a Gibbs measure with potential function $N\bar{U}_N$.

Lemma A.1 (Stationary measure for (12)). *The measure $\tilde{\pi}$ invariant for the dynamics in (12) is given as*

$$\tilde{\pi}(d\tilde{z}, d\tilde{v}) \propto \exp\left(-N\bar{U}_N(\tilde{z}) - \frac{1}{2}\|\tilde{v}\|^2\right) d\tilde{z}d\tilde{v}, \quad (13)$$

for all $\tilde{z}, \tilde{v} \in \mathbb{R}^{d_z}$.

This result follows directly by observing the rescaling given in Proposition A.1 and the standard form of the stationary measure for underdamped Langevin diffusions. We now show that \bar{U}_N is μ -strongly convex under H1.

Lemma A.2 (Strong convexity of \bar{U}_N). *Under H1, the function $\bar{U}_N : \mathbb{R}^{d_\theta + Nd_x} \rightarrow \mathbb{R}$ as defined in (11) is μ -strongly convex*

$$\langle z - z', \nabla \bar{U}_N(z) - \nabla \bar{U}_N(z') \rangle \geq \mu \|z - z'\|^2,$$

for all $z, z' \in \mathbb{R}^{d_\theta + Nd_x}$ and $N \in \mathbb{N}$.

Proof. Let

$$z = (z_\theta, z_1, \dots, z_N), \quad z' = (z'_\theta, z'_1, \dots, z'_N).$$

From

$$\bar{U}_N(z) = \frac{1}{N} \sum_{i=1}^N U(z_\theta, \sqrt{N} z_i),$$

we have

$$\nabla_{z_\theta} \bar{U}_N(z) = \frac{1}{N} \sum_{i=1}^N \nabla_{\theta} U(z_\theta, \sqrt{N} z_i), \quad \nabla_{z_i} \bar{U}_N(z) = \frac{1}{\sqrt{N}} \nabla_x U(z_\theta, \sqrt{N} z_i).$$

Hence

$$\langle z - z', \nabla \bar{U}_N(z) - \nabla \bar{U}_N(z') \rangle = \frac{1}{N} \sum_{i=1}^N \langle z_\theta - z'_\theta, \Delta_{\theta,i} \rangle + \frac{1}{\sqrt{N}} \sum_{i=1}^N \langle z_i - z'_i, \Delta_{x,i} \rangle,$$

where

$$\Delta_{\theta,i} := \nabla_{\theta} U(z_\theta, \sqrt{N} z_i) - \nabla_{\theta} U(z'_\theta, \sqrt{N} z'_i),$$

$$\Delta_{x,i} := \nabla_x U(z_\theta, \sqrt{N} z_i) - \nabla_x U(z'_\theta, \sqrt{N} z'_i).$$

Now apply Assumption H1 to the two points

$$(z_\theta, \sqrt{N} z_i), \quad (z'_\theta, \sqrt{N} z'_i).$$

For each i ,

$$\langle z_\theta - z'_\theta, \Delta_{\theta,i} \rangle + \sqrt{N} \langle z_i - z'_i, \Delta_{x,i} \rangle \geq \mu (\|z_\theta - z'_\theta\|^2 + N \|z_i - z'_i\|^2).$$

Divide by N and sum over i :

$$\langle z - z', \nabla \bar{U}_N(z) - \nabla \bar{U}_N(z') \rangle \geq \mu \|z_\theta - z'_\theta\|^2 + \mu \sum_{i=1}^N \|z_i - z'_i\|^2 = \mu \|z - z'\|^2.$$

So \bar{U}_N is μ -strongly convex. \square

Next, we show that the function \bar{U}_N is L -gradient Lipschitz.

Lemma A.3 (Gradient Lipschitzness of \bar{U}_N). *Under H2, the function $\bar{U}_N : \mathbb{R}^{d_\theta + Nd_x} \rightarrow \mathbb{R}$ as defined in (11) is L -gradient Lipschitz*

$$\|\nabla \bar{U}_N(z) - \nabla \bar{U}_N(z')\| \leq L \|z - z'\|,$$

for all $z, z' \in \mathbb{R}^{d_\theta + Nd_x}$ and $N \in \mathbb{N}$.

Proof. Let $z = (z_\theta, z_1, \dots, z_N)$ and $z' = (z'_\theta, z'_1, \dots, z'_N)$. Then

$$\begin{aligned} \|\nabla \bar{U}_N(z) - \nabla \bar{U}_N(z')\|^2 &= \left\| \frac{1}{N} \sum_{i=1}^N \left(\nabla_{\theta} U(z_\theta, \sqrt{N} z_i) - \nabla_{\theta} U(z'_\theta, \sqrt{N} z'_i) \right) \right\|^2 \\ &\quad + \frac{1}{N} \sum_{i=1}^N \left\| \nabla_x U(z_\theta, \sqrt{N} z_i) - \nabla_x U(z'_\theta, \sqrt{N} z'_i) \right\|^2. \end{aligned}$$

Using the fact that $\|\cdot\|^2$ is a convex function and Jensen's inequality for the first term, we obtain

$$\begin{aligned} \|\nabla \bar{U}_N(z) - \nabla \bar{U}_N(z')\|^2 &\leq \frac{1}{N} \sum_{i=1}^N \left\| \nabla_{\theta} U(z_\theta, \sqrt{N} z_i) - \nabla_{\theta} U(z'_\theta, \sqrt{N} z'_i) \right\|^2 \\ &\quad + \frac{1}{N} \sum_{i=1}^N \left\| \nabla_x U(z_\theta, \sqrt{N} z_i) - \nabla_x U(z'_\theta, \sqrt{N} z'_i) \right\|^2. \end{aligned}$$

Using H2, we have

$$\|\nabla \bar{U}_N(z) - \nabla \bar{U}_N(z')\|^2 \leq \frac{L^2}{N} \sum_{i=1}^N (\|z_\theta - z'_\theta\|^2 + N\|z_i - z'_i\|^2) = L^2 \|z - z'\|^2,$$

which completes the proof. \square

B Equivalence of algorithms

We prove in Proposition A.1 that the KIPLD can be rewritten as a single underdamped Langevin diffusion evolving in $\mathbb{R}^{d_\theta + Nd_x}$. This brings the natural question about the algorithms we derived, namely, KIPLMC1 and KIPLMC2, which are discretisations of the KIPLD, and how they relate to the standard discretisation schemes the rescaled diffusion in (12). We show below that the standard discretisations of (12) are precisely the KIPLMC1 and KIPLMC2 algorithms we defined in Section 3. This will later allow us to leverage existing results on the convergence of these standard discretisation schemes to obtain convergence results for our algorithms.

B.1 KIMPLC1

We show below the exponential integrator algorithm, presented in Dalalyan and Riou-Durand [20], for our diffusion (KIPLD) matches the KIPLMC1 algorithm we defined in Section 3.

Proposition A.2. *Let the sequence $(\tilde{Z}_k, \tilde{V}_k^z)_{k \geq 0}$ be the exponential-integrator discretisation of the rescaled underdamped diffusion (12) with friction parameter $\tilde{\gamma} = \sqrt{N}\gamma$ and step-size $\tilde{\eta} = \eta/\sqrt{N}$. Define the unscaled variables by*

$$\begin{aligned} \tilde{\theta}_k &= \theta_k, & \tilde{X}_k^i &= N^{-1/2} X_k^i, \\ \tilde{V}_k^\theta &= \sqrt{N} V_k^\theta, & \tilde{V}_k^{x_i} &= V_k^{x_i}, \end{aligned}$$

for each $i \in [N]$. Then, after the corresponding rescaling of the Gaussian noise variables, the resulting recursion in $(\theta_k, X_k^i, V_k^\theta, V_k^{x_i})_{i \in [N]}$ coincides exactly with the KIPLMC1 scheme defined in Section 3.1.

Proof. Let us recall that, by Proposition A.1, we can rewrite (KIPLD) as the standard underdamped SDE

$$\begin{aligned} d\tilde{\mathbf{Z}}_t &= \tilde{\mathbf{V}}_t^z dt, \\ d\tilde{\mathbf{V}}_t^z &= -\tilde{\gamma} \tilde{\mathbf{V}}_t^z dt - N \nabla_z \bar{U}_N(\tilde{\mathbf{Z}}_t) dt + \sqrt{2\tilde{\gamma}} d\tilde{\mathbf{B}}_t, \end{aligned}$$

where $\tilde{\gamma} = \sqrt{N}\gamma$ is the friction parameter and we also implicitly adjust its initial conditioned to be rescaled. We discretise this diffusion using the exponential integrator scheme (termed KLMC1) developed by Dalalyan and Riou-Durand [20]. In order to do this, define a sequence of functions $\tilde{\psi}_{k+1}^t = \int_0^t \tilde{\psi}_k^s ds$ where $\tilde{\psi}_0^t = e^{-\tilde{\gamma}t}$. With this definition, the exponential integrator scheme with step-size $\tilde{\eta}$ is defined as

$$\begin{aligned} \tilde{Z}_{k+1} &= \tilde{Z}_k + \tilde{\psi}_1^{\tilde{\eta}} \tilde{V}_k - \tilde{\psi}_2^{\tilde{\eta}} N \nabla_z \bar{U}_N(\tilde{Z}_k) + \sqrt{2\tilde{\gamma}} \zeta'_{k+1} \\ \tilde{V}_{k+1} &= \tilde{\psi}_0^{\tilde{\eta}} \tilde{V}_k - \tilde{\psi}_1^{\tilde{\eta}} N \nabla_z \bar{U}_N(\tilde{Z}_k) + \sqrt{2\tilde{\gamma}} \zeta_{k+1}, \end{aligned}$$

where the stacked vector $[(\zeta_k)_1, \dots, (\zeta_k)_{d_z}, (\zeta'_k)_1, \dots, (\zeta'_k)_{d_z}]^\top$ is a centred Gaussian random variable with covariance $\tilde{C} \otimes I_{d_z}$, where \tilde{C} is given by

$$\tilde{C} = \int_0^{\tilde{\eta}} \begin{bmatrix} \tilde{\psi}_0^t \\ \tilde{\psi}_1^t \end{bmatrix} \begin{bmatrix} \tilde{\psi}_0^t & \tilde{\psi}_1^t \end{bmatrix} dt.$$

Written explicitly via the definition of $\tilde{\psi}_i^t$, we have,

$$\tilde{C} = \frac{1}{2\tilde{\gamma}} \begin{pmatrix} (1 - e^{-2\tilde{\gamma}\tilde{\eta}}) & \frac{(e^{-\tilde{\gamma}\tilde{\eta}} - 1)^2}{\tilde{\gamma}} \\ \frac{(e^{-\tilde{\gamma}\tilde{\eta}} - 1)^2}{\tilde{\gamma}} & \frac{2\tilde{\gamma}\tilde{\eta} + 4e^{-\tilde{\gamma}\tilde{\eta}} - e^{-2\tilde{\gamma}\tilde{\eta}} - 3}{\tilde{\gamma}^2} \end{pmatrix}$$

Let us now relate the matrix \tilde{C} to the matrix we have defined in (7) for the KIPLMC1 scheme. Written explicitly with the definitions in Section 3.1, KIPLMC1 instead defines functions $\psi_0^\eta = e^{-\gamma\eta}$ and $\psi_{i+1}^\eta = \int_0^\eta \psi_i^t dt$, and the covariance matrix in (7) is given as

$$C = \frac{1}{2\gamma} \begin{pmatrix} (1 - e^{-2\gamma\eta}) & \frac{(e^{-\gamma\eta} - 1)^2}{\gamma} \\ \frac{(e^{-\gamma\eta} - 1)^2}{\gamma} & \frac{2\gamma\eta + 4e^{-\gamma\eta} - e^{-2\gamma\eta} - 3}{\gamma^2} \end{pmatrix}.$$

Recall that the stacked vector $[(\varepsilon_k)_1, (\varepsilon'_k)_1, (\varepsilon_k)_2, (\varepsilon'_k)_2, \dots, ((\varepsilon_k)_{d_z}, (\varepsilon'_k)_{d_z})]^\top$ is a centred Gaussian random variable with covariance $C \otimes I_{d_z}$ as defined in Section 3.1. Note the relation between \tilde{C} and C is given by

$$\tilde{C} = \begin{pmatrix} N^{-\frac{1}{2}}C_{11} & N^{-1}C_{12} \\ N^{-1}C_{21} & N^{-\frac{3}{2}}C_{22} \end{pmatrix}.$$

Hence, we recover

$$\begin{aligned} \zeta_k &= (N)^{-\frac{1}{4}} (\varepsilon_k^0, \dots, \varepsilon_k^N)^\top, \\ \zeta'_k &= (N)^{-\frac{3}{4}} (\varepsilon_k^{0,\prime}, \dots, \varepsilon_k^{N,\prime})^\top. \end{aligned}$$

We first write the full exponential-integrator scheme coordinatewise, without yet substituting the relations between $\tilde{\eta}$ and η or between the rescaled and original variables. This gives

$$\begin{aligned} \tilde{\theta}_{k+1} &= \tilde{\theta}_k + \tilde{\psi}_1^{\tilde{\eta}} \tilde{V}_k^\theta - \tilde{\psi}_2^{\tilde{\eta}} N \nabla_\theta \bar{U}_N(\tilde{Z}_k) + \sqrt{2\tilde{\gamma}} (\zeta'_k)^0, \\ \tilde{X}_{k+1}^i &= \tilde{X}_k^i + \tilde{\psi}_1^{\tilde{\eta}} \tilde{V}_k^{x_i} - \tilde{\psi}_2^{\tilde{\eta}} N \nabla_{z_i} \bar{U}_N(\tilde{Z}_k) + \sqrt{2\tilde{\gamma}} (\zeta'_k)^i, \\ \tilde{V}_{k+1}^\theta &= \tilde{\psi}_0^{\tilde{\eta}} \tilde{V}_k^\theta - \tilde{\psi}_1^{\tilde{\eta}} N \nabla_\theta \bar{U}_N(\tilde{Z}_k) + \sqrt{2\tilde{\gamma}} (\zeta_k)^0, \\ \tilde{V}_{k+1}^{x_i} &= \tilde{\psi}_0^{\tilde{\eta}} \tilde{V}_k^{x_i} - \tilde{\psi}_1^{\tilde{\eta}} N \nabla_{z_i} \bar{U}_N(\tilde{Z}_k) + \sqrt{2\tilde{\gamma}} (\zeta_k)^i, \end{aligned}$$

where the noise variables $(\zeta_k)^0$, $(\zeta'_k)^0$, $(\zeta_k)^i$ and $(\zeta'_k)^i$ are the appropriate coordinates of ζ_k and ζ'_k respectively. Now recall from Proposition A.1 that $\tilde{\gamma} = \sqrt{N}\gamma$, and choose $\tilde{\eta} = \eta/\sqrt{N}$. Then

$$\tilde{\psi}_0^{\tilde{\eta}} = e^{-\gamma\eta} = \psi_0^\eta, \quad \tilde{\psi}_1^{\tilde{\eta}} = \frac{1}{\gamma\sqrt{N}}(1 - e^{-\gamma\eta}) = \frac{\psi_1^\eta}{\sqrt{N}}, \quad \tilde{\psi}_2^{\tilde{\eta}} = \frac{1}{\gamma N}(\eta - \frac{1}{\gamma}(1 - e^{-\gamma\eta})) = \frac{\psi_2^\eta}{N}.$$

Using also the identities

$$\begin{aligned} N \nabla_\theta \bar{U}_N(\tilde{Z}_k) &= \sum_{i=1}^N \nabla_\theta U(\tilde{\theta}_k, \sqrt{N} \tilde{X}_k^i), \\ N \nabla_{z_i} \bar{U}_N(\tilde{Z}_k) &= \sqrt{N} \nabla_{x_i} U(\tilde{\theta}_k, \sqrt{N} \tilde{Z}_k^i), \end{aligned} \tag{14}$$

together with $\tilde{\theta}_k = \theta_k$, $\tilde{X}_k^i = N^{-1/2} X_k^i$, $\tilde{V}_k^\theta = \sqrt{N} V_k^\theta$, $\tilde{V}_k^{x_i} = V_k^{x_i}$, $(\zeta_k)^0 = N^{-1/4} \varepsilon_k^0$, $(\zeta'_k)^0 = N^{-3/4} \varepsilon_k^{0,\prime}$, $(\zeta_k)^i = N^{-1/4} \varepsilon_k^i$, and $(\zeta'_k)^i = N^{-3/4} \varepsilon_k^{i,\prime}$, we obtain for the θ -coordinates

$$\begin{aligned} \theta_{k+1} &= \theta_k + \frac{\psi_1^\eta}{\sqrt{N}} \tilde{V}_k^\theta - \frac{\psi_2^\eta}{N} \sum_{i=1}^N \nabla_\theta U(\theta_k, X_k^i) + \sqrt{\frac{2\gamma}{N}} \varepsilon_k^{0,\prime}, \\ \tilde{V}_{k+1}^\theta &= \psi_0^\eta \tilde{V}_k^\theta - \frac{\psi_1^\eta}{\sqrt{N}} \sum_{i=1}^N \nabla_\theta U(\theta_k, X_k^i) + \sqrt{2\gamma} \varepsilon_k^0. \end{aligned}$$

Since $\tilde{V}_k^\theta = \sqrt{N}V_k^\theta$, substituting this relation into the first line and dividing the second line by \sqrt{N} yields

$$\begin{aligned}\theta_{k+1} &= \theta_k + \psi_1^\eta V_k^\theta - \frac{\psi_2^\eta}{N} \sum_{i=1}^N \nabla_\theta U(\theta_k, X_k^i) + \sqrt{\frac{2\gamma}{N}} \varepsilon_k^{0,\prime}, \\ V_{k+1}^\theta &= \psi_0^\eta V_k^\theta - \frac{\psi_1^\eta}{N} \sum_{i=1}^N \nabla_\theta U(\theta_k, X_k^i) + \sqrt{\frac{2\gamma}{N}} \varepsilon_k^0.\end{aligned}$$

For each particle coordinate $i \in [N]$, the same substitutions give

$$\begin{aligned}\tilde{X}_{k+1}^i &= \tilde{X}_k^i + \frac{\psi_1^\eta}{\sqrt{N}} V_k^{x_i} - \frac{\psi_2^\eta}{\sqrt{N}} \nabla_x U(\theta_k, X_k^i) + \sqrt{\frac{2\gamma}{N}} \varepsilon_k^{i,\prime}, \\ V_{k+1}^{x_i} &= \psi_0^\eta V_k^{x_i} - \psi_1^\eta \nabla_x U(\theta_k, X_k^i) + \sqrt{2\gamma} \varepsilon_k^i.\end{aligned}$$

Finally, multiplying the first equation by \sqrt{N} , i.e. using $X_k^i = \sqrt{N}\tilde{X}_k^i$, yields

$$\begin{aligned}X_{k+1}^i &= X_k^i + \psi_1^\eta V_k^{x_i} - \psi_2^\eta \nabla_x U(\theta_k, X_k^i) + \sqrt{2\gamma} \varepsilon_k^{i,\prime}, \\ V_{k+1}^{x_i} &= \psi_0^\eta V_k^{x_i} - \psi_1^\eta \nabla_x U(\theta_k, X_k^i) + \sqrt{2\gamma} \varepsilon_k^i.\end{aligned}$$

Together with the θ -update above, this is precisely the KIPLMC1 scheme. \square

B.2 KIPLMC2

Proposition A.3. *Let $(\tilde{Z}_k, \tilde{V}_k^z)_{k \geq 0}$ be the OBABO discretisation of the rescaled underdamped diffusion (12) with friction parameter $\tilde{\gamma} = \sqrt{N}\gamma$ and step-size $\tilde{\eta} = \eta/\sqrt{N}$. Define the unscaled variables by*

$$\begin{aligned}\tilde{\theta}_k &= \theta_k, & \tilde{X}_k^i &= N^{-1/2} X_k^i, \\ \tilde{V}_k^\theta &= \sqrt{N} V_k^\theta, & \tilde{V}_k^{x_i} &= V_k^{x_i},\end{aligned}$$

for each $i \in [N]$. Then the resulting recursion in $(\theta_k, X_k^i, V_k^\theta, V_k^{x_i})_{i \in [N]}$ coincides exactly with the KIPLMC2 scheme defined in Algorithm 2.

Proof. In this case we again apply Proposition A.1 to apply the OBABO results from Monmarché [41] for the standard underdamped diffusion, to our own. Let us recall the standard form, given in Proposition A.1 with $\tilde{\gamma} = \sqrt{N}\gamma$,

$$\begin{aligned}d\tilde{\mathbf{Z}}_t &= \tilde{\mathbf{V}}_t^z dt, \\ d\tilde{\mathbf{V}}_t^z &= -\tilde{\gamma} \tilde{\mathbf{V}}_t^z dt - N \nabla_z \bar{U}_N(\tilde{\mathbf{Z}}_t) dt + \sqrt{2\tilde{\gamma}} d\tilde{\mathbf{B}}_t,\end{aligned}$$

This diffusion is discretised with the OBABO scheme with step-size $\tilde{\eta}$, to obtain,

$$\begin{aligned}\tilde{Z}_{k+1} &= \tilde{Z}_k + \tilde{\eta} \left(\delta \tilde{V}_k + \sqrt{1 - \delta^2} \xi_{k+1} \right) - \frac{\tilde{\eta}^2}{2} N \nabla_z \bar{U}_N(\tilde{Z}_k) \\ \tilde{V}_{k+1} &= \delta^2 \tilde{V}_k + \sqrt{1 - \delta^2} (\delta \xi_{k+1} + \xi'_{k+1}) - \frac{\tilde{\eta} \delta}{2} N (\nabla_z \bar{U}_N(\tilde{Z}_k) + \nabla_z \bar{U}_N(\tilde{Z}_{k+1})),\end{aligned}$$

where we recall that $\delta = e^{-\tilde{\gamma}\tilde{\eta}/2}$. Let us begin at looking at the discretisation coordinatewise in the scaled case,

$$\begin{aligned}\tilde{\theta}_{k+1} &= \tilde{\theta}_k + \tilde{\eta} \left(\delta \tilde{V}_k^\theta + \sqrt{1 - \delta^2} \xi_{k+1}^0 \right) - \frac{\tilde{\eta}^2}{2} N \nabla_\theta \bar{U}_N(\tilde{Z}_k), \\ \tilde{X}_{k+1}^i &= \tilde{X}_k^i + \tilde{\eta} \left(\delta \tilde{V}_k^{x_i} + \sqrt{1 - \delta^2} \xi_{k+1}^i \right) - \frac{\tilde{\eta}^2}{2} N \nabla_{z_i} \bar{U}_N(\tilde{Z}_k), \\ \tilde{V}_{k+1}^\theta &= \delta^2 \tilde{V}_k^\theta + \sqrt{1 - \delta^2} (\delta \xi_{k+1}^0 + \xi_{k+1}^{0,\prime}) - \frac{\tilde{\eta} \delta}{2} N (\nabla_\theta \bar{U}_N(\tilde{Z}_k) + \nabla_\theta \bar{U}_N(\tilde{Z}_{k+1})), \\ \tilde{V}_{k+1}^{x_i} &= \delta^2 \tilde{V}_k^{x_i} + \sqrt{1 - \delta^2} (\delta \xi_{k+1}^i + \xi_{k+1}^{i,\prime}) - \frac{\tilde{\eta} \delta}{2} N (\nabla_{z_i} \bar{U}_N(\tilde{Z}_k) + \nabla_{z_i} \bar{U}_N(\tilde{Z}_{k+1})).\end{aligned}$$

We now proceed to rescaling the algorithm by observing that $\tilde{\delta} = \delta$ and recalling that $\tilde{\psi}_0^{\tilde{\eta}} = \psi_0^\eta$. Using this, $\tilde{\eta} = \eta/\sqrt{N}$ and $\tilde{\gamma} = \sqrt{N}\gamma$ and the identities (14), we obtain for the θ -coordinates,

$$\begin{aligned}\theta_{k+1} &= \theta_k + \frac{\eta}{\sqrt{N}} \left(\delta \tilde{V}_k^\theta + \sqrt{1 - \delta^2} \xi_{k+1} \right) - \frac{\eta^2}{2N} \sum_{i=1}^N \nabla_\theta U(\theta_k, X_k^i) \\ \tilde{V}_{k+1}^\theta &= \delta^2 \tilde{V}_k^\theta + \sqrt{1 - \delta^2} (\delta \xi_{k+1} + \xi'_{k+1}) - \frac{\eta \delta}{2\sqrt{N}} \sum_{i=1}^N \left(\nabla_\theta U(\theta_k, X_k^i) + \nabla_\theta U(\theta_{k+1}, X_{k+1}^i) \right),\end{aligned}$$

Substituting in the relationship $\tilde{V}_k^\theta = \sqrt{N}V_k^\theta$ and $\tilde{X}_k^i = X_k^i/\sqrt{N}$, we obtain,

$$\begin{aligned}\theta_{k+1} &= \theta_k + \eta \left(\delta V_k^\theta + \sqrt{\frac{1 - \delta^2}{N}} \xi_{k+1} \right) - \frac{\eta^2}{2N} \sum_{i=1}^N \nabla_\theta U(\theta_k, X_k^i) \\ V_{k+1}^\theta &= \delta^2 V_k^\theta + \sqrt{\frac{1 - \delta^2}{N}} (\delta \xi_{k+1} + \xi'_{k+1}) - \frac{\eta \delta}{2N} \sum_{i=1}^N \left(\nabla_\theta U(\theta_k, X_k^i) + \nabla_\theta U(\theta_{k+1}, X_{k+1}^i) \right).\end{aligned}$$

For the particles $i \in [N]$, the same substitutions give,

$$\begin{aligned}\tilde{X}_{k+1}^i &= \tilde{X}_k^i + \frac{\eta}{\sqrt{N}} \left(\delta V_k^{x_i} + \sqrt{1 - \delta^2} \xi_{k+1}^i \right) - \frac{\eta^2}{2N} \nabla_{x_i} U(\theta_k, \sqrt{N} \tilde{X}_k^i), \\ V_{k+1}^{x_i} &= \delta^2 V_k^{x_i} + \sqrt{1 - \delta^2} (\delta \xi_{k+1}^i + \xi_{k+1}^{i'}) - \frac{\eta \delta}{2\sqrt{N}} (\nabla_{x_i} U(\theta_k, \sqrt{N} \tilde{X}_k^i) + \nabla_{x_i} U(\theta_{k+1}, \sqrt{N} \tilde{X}_{k+1}^i)).\end{aligned}$$

Finally, using $X_k^i = \sqrt{N} \tilde{X}_k^i$, we recover,

$$\begin{aligned}X_{k+1}^i &= X_k^i + \eta \left(\delta V_k^{x_i} + \sqrt{1 - \delta^2} \xi_{k+1} \right) - \frac{\eta^2}{2} \nabla_x U(\theta_k, X_k^i) \\ V_{k+1}^{x_i} &= \delta^2 V_k^{x_i} + \sqrt{1 - \delta^2} (\delta \xi_{k+1} + \xi'_{k+1}) - \frac{\eta \delta}{2} \left(\nabla_x U(\theta_k, X_k^i) + \nabla_x U(\theta_{k+1}, X_{k+1}^i) \right).\end{aligned}$$

This shows that the OBABO discretisation of the rescaled diffusion, with step-size $\tilde{\eta} = \eta/\sqrt{N}$, is precisely the KIPLMC2 scheme. \square

Remark A.1. *The results in Propositions A.1–A.3 significantly streamline our proofs, since they allow us to connect KIPLD and our methods KIPLMC1 and KIPLMC2 to the standard underdamped diffusion and its discretisations, for which there is a rich literature of results that we can apply.*

C Proofs of main results

C.1 Proof of Proposition 1

Given Proposition A.1, the system (12) has a stationary measure given by the density

$$\tilde{\pi}(z, \bar{v}) \propto \exp \left(-N \bar{U}_N(z) - \frac{1}{2} \|\bar{v}\|^2 \right),$$

where \bar{U}_N is given in (11). Let us now look at θ -marginal of this density, which can be written as

$$\pi_\Theta(\theta) \propto \int e^{-\sum_{i=1}^N U(\theta, \sqrt{N} z_i) - \frac{1}{2} \|\bar{v}\|^2} dz_x d\bar{v}.$$

where $z_x = (z_1, \dots, z_N) \in \mathbb{R}^{Nd_x}$. Note now that, integrating out \bar{v} , using a change of variables $x'_i = \sqrt{N} z_i$, and setting $x' = (x'_1, \dots, x'_N)$, we have

$$\pi_\Theta(\theta) \propto \int_{\mathbb{R}^{Nd_x}} e^{-\sum_{i=1}^N U(\theta, x'_i)} dx' \propto \left(\int_{\mathbb{R}^{d_x}} e^{-U(\theta, x')} dx' \right)^N = \exp(N \log p_\theta(y)),$$

since $p_\theta(y) = \int e^{-U(\theta, x)} dx$ by definition, where $U(\theta, x) = -\log p_\theta(x, y)$.

C.2 Proof of Proposition 2

Note that, by H1, $U(\theta, x)$ is jointly μ -strongly convex. Let $\kappa(\theta) = -\log p_\theta(y)$. Using the Prékopa-Leindler inequality for strongly log-concave distributions [46, Theorem 3.8], we can see that

$$\langle \theta - \theta', \nabla \kappa(\theta) - \nabla \kappa(\theta') \rangle \geq \mu \|\theta - \theta'\|^2.$$

The bound now follows using Lemma A.8 from Altschuler and Chewi [5].

C.3 Proof of Proposition 3

By Proposition A.1, the rescaled process $(\tilde{\mathbf{Z}}_t, \tilde{\mathbf{V}}_t^z)$ solves the standard underdamped SDE

$$\begin{aligned} d\tilde{\mathbf{Z}}_t &= \tilde{\mathbf{V}}_t^z dt, \\ d\tilde{\mathbf{V}}_t^z &= -\tilde{\gamma} \tilde{\mathbf{V}}_t^z dt - \nabla N \bar{U}_N(\tilde{\mathbf{Z}}_t) dt + \sqrt{2\tilde{\gamma}} d\tilde{\mathbf{B}}_t, \end{aligned} \tag{15}$$

with $\tilde{\gamma} = \sqrt{N}\gamma$. By Lemmas A.2 and A.3, \bar{U}_N is μ -strongly convex and L -gradient-Lipschitz, hence $N\bar{U}_N$ is $N\mu$ -strongly convex and NL -gradient-Lipschitz. Define

$$\tilde{\mu} := N\mu, \quad \tilde{L} := NL.$$

The condition $\gamma \geq \sqrt{\mu + L}$ implies

$$\tilde{\gamma} = \sqrt{N}\gamma \geq \sqrt{N(\mu + L)} = \sqrt{\tilde{\mu} + \tilde{L}}.$$

Therefore Theorem 1 in Dalalyan and Riou-Durand [20] applies to (15) and yields, for $s \geq 0$,

$$W_2(\mathcal{L}(\tilde{\mathbf{Z}}_s), \tilde{\pi}_{\mathbf{Z}}) \leq \sqrt{2} \exp\left(-\frac{\tilde{\mu}}{\tilde{\gamma}} s\right) W_2(\mathcal{L}(\tilde{\mathbf{Z}}_0), \tilde{\pi}_{\mathbf{Z}}).$$

where $\tilde{\pi}_{\mathbf{Z}}$ is the $\tilde{\mathbf{Z}}$ -marginal of $\tilde{\pi}$ (Lemma A.1).

Now relate rescaled and original time: by definition,

$$\tilde{\mathbf{Z}}_{t/\sqrt{N}} = (\boldsymbol{\theta}_t, N^{-1/2} \mathbf{X}_t^1, \dots, N^{-1/2} \mathbf{X}_t^N)^\top.$$

Hence the θ -component of $\tilde{\mathbf{Z}}_{t/\sqrt{N}}$ is $\boldsymbol{\theta}_t$, and the θ -marginal of $\tilde{\pi}_{\mathbf{Z}}$ is π_Θ . We note

$$W_2(\mathcal{L}(\boldsymbol{\theta}_t), \pi_\Theta) \leq W_2(\mathcal{L}(\tilde{\mathbf{Z}}_{t/\sqrt{N}}), \tilde{\pi}_{\mathbf{Z}}).$$

Using $s = t/\sqrt{N}$ gives

$$\frac{\tilde{\mu}}{\tilde{\gamma}} \frac{t}{\sqrt{N}} = \frac{N\mu}{\sqrt{N}\gamma} \frac{t}{\sqrt{N}} = \frac{\mu}{\gamma} t.$$

Therefore

$$W_2(\mathcal{L}(\boldsymbol{\theta}_t), \pi_\Theta) \leq \sqrt{2} \exp\left(-\frac{\mu}{\gamma} t\right) W_2(\mathcal{L}(\tilde{\mathbf{Z}}_0), \tilde{\pi}_{\mathbf{Z}}).$$

Finally, with $\bar{Z}_\star \sim \tilde{\pi}_{\mathbf{Z}}$,

$$W_2(\mathcal{L}(\tilde{\mathbf{Z}}_0), \tilde{\pi}_{\mathbf{Z}}) \leq \mathbb{E}[\|\tilde{\mathbf{Z}}_0 - \bar{Z}_\star\|^2]^{1/2},$$

which is exactly the stated bound (up to the same notation $\tilde{\mathbf{Z}}_0 \equiv \mathbf{Z}_0$ used in the proposition).

C.4 Proof of Theorem 1

By Proposition A.1, we can rewrite KIPLD as the standard underdamped diffusion with stationary measure

$$\tilde{\pi}(z, v) \propto e^{-N\bar{U}_N(z) - \|v\|^2/2}.$$

We will now look at the standard kinetic Langevin Monte Carlo discretisation of the SDE and show that this scheme coincides with KIPLMC1 to utilize the bounds in Dalalyan and Riou-Durand [20] directly.

Let us write the Exponential Integrator discretisation of this scheme as we do in B.1,

$$\begin{aligned}\tilde{Z}_{n+1} &= \tilde{Z}_n + \tilde{\psi}_1^{\tilde{\eta}} \tilde{V}_n^z - \tilde{\psi}_2^{\tilde{\eta}} N \nabla \bar{U}_N(\tilde{Z}_n) + \sqrt{2\tilde{\gamma}} \zeta'_{n+1}, \\ \tilde{V}_{n+1}^z &= \tilde{\psi}_0^{\tilde{\eta}} \tilde{V}_n^z - \tilde{\psi}_1^{\tilde{\eta}} N \nabla \bar{U}_N(\tilde{Z}_n) + \sqrt{2\tilde{\gamma}} \zeta_{n+1}.\end{aligned}\tag{16}$$

Since the function $z \mapsto N\bar{U}_N(z)$ is $N\mu$ strongly convex and NL -gradient-Lipschitz, for $\tilde{\gamma} \geq \sqrt{N\mu + NL}$ and $\tilde{\eta} \leq \mu/(4\tilde{\gamma}L)$, Dalalyan and Riou-Durand [20, Theorem 2] directly implies that

$$W_2(\nu_n, \tilde{\pi}) \leq \sqrt{2\mathbb{E}[\|Z_0 - \bar{Z}_*\|^2]^{1/2}} \left(1 - \frac{0.75\tilde{\mu}\tilde{\eta}}{\tilde{\gamma}}\right)^n + \frac{\tilde{\eta}\tilde{L}}{\tilde{\mu}} \sqrt{2d_z},$$

where ν_n denotes the law of the discretisation (16) at time n , $\tilde{\pi}$ the stationary measure given in Lemma A.1 and $\bar{Z}_* \sim \tilde{\pi}$. We now recall from B.1, that $\tilde{\eta} = \eta/\sqrt{N}$ and $\tilde{\gamma} = \sqrt{N}\gamma$, from which we obtain,

$$W_2(\nu_n, \tilde{\pi}) \leq C_1 \left(1 - \frac{0.75\mu\eta}{\gamma}\right)^n + \eta C_2,$$

where,

$$\begin{aligned}C_1 &= \sqrt{2\mathbb{E}[\|Z_0 - \bar{Z}_*\|^2]^{1/2}}, \quad \bar{Z}_* \sim \tilde{\pi} \\ C_2 &= \sqrt{2} \frac{L}{\mu} \sqrt{\frac{d_z}{N}}.\end{aligned}$$

Let us now recall that $\mathcal{L}(\theta_n)$ and π_Θ are restrictions of the measures ν_n and $\tilde{\pi}$ respectively. Applying this and a triangle inequality, we obtain,

$$\begin{aligned}\mathbb{E}[\|\theta_n - \bar{\theta}_*\|^2]^{1/2} &= W_2(\mathcal{L}(\theta_n), \delta_{\bar{\theta}_*}) \\ &\leq W_2(\mathcal{L}(\theta_n), \pi_\Theta) + W_2(\pi_\Theta, \delta_{\bar{\theta}_*}) \\ &\leq C_1 \left(1 - \frac{0.75\mu\eta}{\gamma}\right)^n + \eta C_2 + \sqrt{\frac{C_3}{N}},\end{aligned}$$

where the last term is bounded by Proposition 2 with $C_3 = d_\theta/\mu$.

C.5 Proof of Theorem 2

Again, we consider our rescaled standard underdamped diffusion, given by (12) and seek to directly apply the results from Monmarché [41] for our scheme.

We now write the splitting scheme as in B.2,

$$\begin{aligned}\tilde{Z}_{n+1} &= \tilde{Z}_n + \tilde{\eta}(\delta\tilde{V}_n^z + \sqrt{1 - \delta^2}\xi_{n+1}) - \frac{\tilde{\eta}^2}{2} N \nabla \bar{U}_N(\tilde{Z}_n) \\ \tilde{V}_{n+1}^z &= \delta^2 \tilde{V}_n^z - \frac{\tilde{\eta}\tilde{\delta}}{2} (N \nabla \bar{U}_N(\tilde{Z}_n) + N \nabla \bar{U}_N(\tilde{Z}_{n+1})) + \sqrt{1 - \delta^2}(\delta\xi_{n+1} + \xi'_{n+1}),\end{aligned}\tag{17}$$

where $\tilde{\delta} = e^{-\tilde{\gamma}\tilde{\eta}/2}$. Using the \tilde{L} -gradient-Lipschitzness and $\tilde{\mu}$ strong convexity of the function $z \mapsto N\bar{U}_N(z)$, we are able to apply Theorem 1 from Monmarché [41]. This result states that, for $\tilde{\gamma} \geq 2\sqrt{\tilde{L}}$ and $\tilde{\eta} \leq N\mu/(33\tilde{\gamma}^3)$,

$$W_2(\nu_n, \tilde{\pi}) \leq \tilde{C}_1 \left(1 - \frac{\tilde{\eta}\tilde{\mu}}{3\tilde{\gamma}}\right)^{n/2} + \tilde{\eta}K_1,$$

where ν_n is now the law of the discretisation (17) at time n , $\tilde{\pi}$ is the stationary measure from Lemma A.1 and,

$$K_1 = \sqrt{2d_z} \frac{6\tilde{\gamma}\tilde{K}}{\tilde{\mu}} \sqrt{3N}(\sqrt{L} \vee \sqrt{L}^{-1}), \quad \tilde{K} = \tilde{L} \left(1 + e^{\tilde{L}\tilde{\eta}^2} \left(\frac{\tilde{\eta}}{6} + \frac{\tilde{\eta}^2\tilde{L}}{24} \right) \right) \left(1 + \frac{\tilde{\eta}\tilde{L}}{2\sqrt{\tilde{\mu}}} \right).$$

Let us now recall from Theorem 2, the defined constants,

$$\tilde{C}_1 = \sqrt{3}(\sqrt{L} \vee \sqrt{L}^{-1}) \mathbb{E}[\|Z_0 - \bar{Z}^*\|^2]^{1/2}, \quad \tilde{C}_2 = \sqrt{2d_z} \frac{6\gamma K}{\mu} \sqrt{3}(\sqrt{L} \vee \sqrt{L}^{-1}),$$

$$K = L \left(1 + e^{L\eta^2} \left(\frac{\eta}{6} + \frac{\eta^2 L}{24} \right) \right) \left(1 + \frac{\eta L}{2\sqrt{\mu}} \right).$$

Further, recall that, $\tilde{\mu} = N\mu$, $\tilde{L} = NL$, $\tilde{\eta} = \eta/\sqrt{N}$ and $\tilde{\gamma} = \sqrt{N}\gamma$. With this we obtain,

$$W_2(\nu_n, \tilde{\pi}) \leq \tilde{C}_1 \left(1 - \frac{\tilde{\eta}N\mu}{3\tilde{\gamma}} \right)^{n/2} + \sqrt{N}\tilde{\eta}\tilde{C}_2.$$

Again, applying the triangle inequality and Proposition 2, gives us,

$$\mathbb{E}[\|\theta_n - \bar{\theta}_*\|^2]^{1/2} \leq \tilde{C}_1 \left(1 - \frac{\eta\mu}{3\gamma} \right)^{n/2} + \eta\tilde{C}_2 + \sqrt{\frac{\tilde{C}_3}{N}},$$

with $C_3 = d_\theta/\mu$.

D Results

D.1 Multi-well Experiment

We include the following multi-well experiment to highlight the advantage of the noised θ dynamics, the core difference between the proposed methods and MPGD [37]. To do this, we consider a synthetic example with

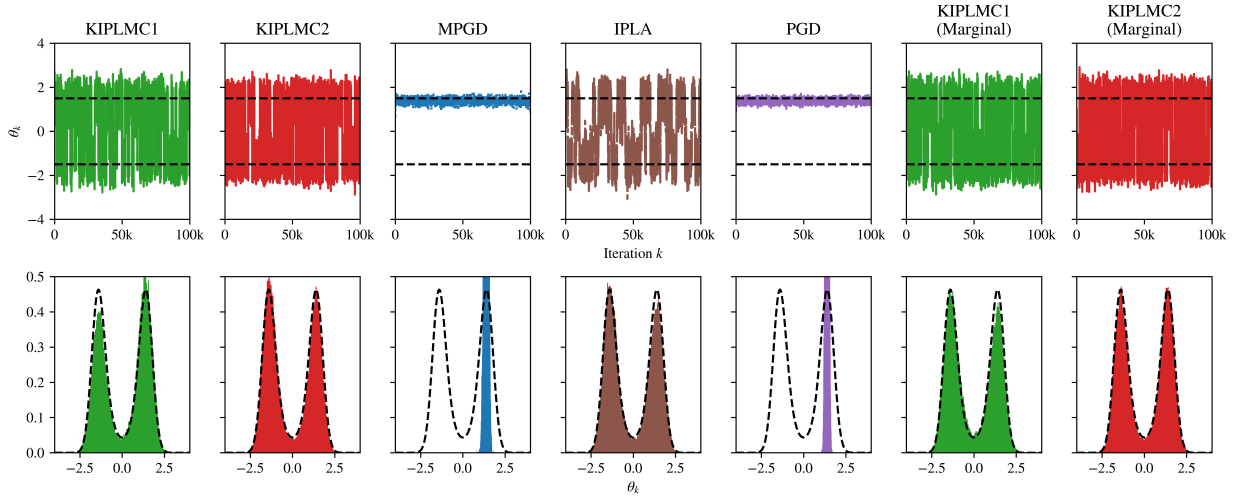


Figure 5: **Multi-well Experiment.** The trace plots for KIPLMC1, KIPLMC2, MPGD, IPLA and PGD on the multi-well experiment, together with density plots. We have shown in black, dashed lines the “true” values of θ_* in the trace plots and the “true” posterior density for θ in the density plots. $N = 10$ and the friction and step-size are optimised for each algorithm.

non-convex posterior. Consider the joint probability density over \mathbb{R} ,

$$p_\theta(x, y) = \mathcal{N}(y; x, \sigma_y^2)p_\theta(x),$$

$$p_\theta(x) = \frac{1}{2}\mathcal{N}(x; -\theta, \sigma_x^2) + \frac{1}{2}\mathcal{N}(x; \theta, \sigma_x^2).$$

One can note that given small enough choices of σ_x and σ_y , as well as, large enough $\bar{\theta}_*$, this density has a multi-modal θ -marginal. Indeed, let us observe that the parameter posterior is given as,

$$p_\theta(y) = \frac{1}{2}\mathcal{N}(y; \theta, \sigma_x^2 + \sigma_y^2) + \frac{1}{2}\mathcal{N}(y; -\theta, \sigma_x^2 + \sigma_y^2).$$

In this case, we seek to show that whilst the MPGD algorithm gets stuck in one of the local minima, the KIPLMC1 algorithm escapes these under the same hyperparameters. For the experiment we generate 1 data-points at $\theta = 1.5$, from which we obtain true $\bar{\theta}_* = \pm 1.5$, and we fix $\sigma_x^2 = 1$ and $\sigma_y^2 = 0.25$. In Fig. 5, we show the trace plots of θ , together with the associated empirical density plots, compared to $\bar{\theta}_*$ and the marginal likelihood $p_\theta(y)$ respectively. For sake of comparison, we also compare the dynamics of KIPLMC1 and KIPLMC2 on the marginal dynamics, i.e. we consider KIPLD to be given simply as

$$d\theta_t = \mathbf{V}_t^\theta dt,$$

$$d\mathbf{V}_t^\theta = -\gamma\mathbf{V}_t^\theta - \nabla_\theta\kappa(\theta)dt + \sqrt{\frac{2\gamma}{N}}d\mathbf{B}_t,$$

for a \mathbb{R}^{d_θ} Brownian motion \mathbf{B}_t and we recall from Proposition 1 that $\kappa(\theta) = -\log p_\theta(y)$. In Fig. 5 we observe that all methods converge close to the true solution, but only the “noised” algorithms KIPLMC1, KIPLMC2 and IPLA successfully have support on both true solutions reliably.

D.2 Computational Cost Comparison

We further perform an additional experiment on the Sec. 5.1 example, to compare MSE against computational cost. Indeed, this allows for more thorough comparisons with the methods, as KIPLMC1 generates correlated noise, KIPLMC2 performs a gradient correction and MPGD does both. Further all these methods require twice as much space in memory, when compared to PGD and IPLA, due to the presence of the momentum variables.

In Fig. 6, we observe the faster initial convergence rate of the momentum based methods, despite their greater computational cost. Further, we observe that the increased cost of noising the θ -dynamics in our proposed methods, is negligible when compared to a second gradient evaluation per iteration, required by MPGD and KIPLMC2.

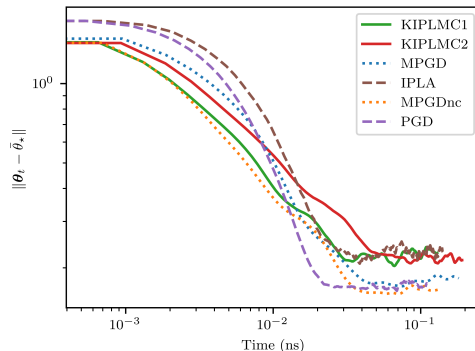


Figure 6: **Runtime Comparison.** We compare the MSE for the synthetic logistic regression experiment performed in Sec. 5.1 with the same hyperparameters $d_x = d_\theta = 3$, $d_y = 100$, $\gamma = 2.2$ and $N = 100$. The results shown are the average of 100 Monte Carlo simulations.

D.3 Area Between Curve Calculation (ABC)

To compare the behaviour of the different algorithms, we employ a measure that quantifies how accurately and quickly each algorithm converges to the true solution, namely the ABC, as in Lim et al. [37]. Consider $c^k : \mathbb{N} \rightarrow \mathbb{R}$ and $c^m : \mathbb{N} \rightarrow \mathbb{R}$ to be the accuracy curves of KIPLMC2 and IPLA respectively, i.e. for $\{\theta_n\}_{n=1}^\infty$ generated by the KIPLMC2 algorithm, $c^k(n) = \|\theta_n - \bar{\theta}^*\|$. The ABC is given as,

$$\sum_{i=1}^M w(i)(c^m(i) - c^k(i)),$$

where M is the total number of time-steps and w acts as a weighting function $w(i) = 2i/(M(M+1))$, matching Kuntz et al. [35]. Hence, the ABC computes a signed, weighted area between the error curves of IPLA and KIPLMC2. In particular, when c^m is dominated by c^k , the ABC is negative, whilst positive in the converse case.

D.4 Error Metrics for the BNN

Recall that the output of our model for latent variable $x = (w, v)$, image features f is,

$$p(l|f, x) \propto \exp \left(\sum_{j=1}^{40} v_{lj} \tanh \left(\sum_{i=1}^{784} w_{ji} f_i \right) \right).$$

To normalise the outputs of the RHS over the labels we apply softmax to the estimates for all l . Denote this as $g(l|f, x)$ and we give the output of the model as

$$\hat{l}(f|x) = \operatorname{argmax}_{l \in \{0,1\}} g(l|f, x).$$

For the BNN in 5.3 we use two metrics to evaluate the performance of our models, which we evaluate on test set of 200 images and labels $\mathcal{Y}_{\text{test}}$. In particular we use a relative error metric, measuring the percentage accuracy on the test set,

$$\frac{1}{|\mathcal{Y}_{\text{test}}|} \sum_{(f,l) \in \mathcal{Y}_{\text{test}}} |l - \hat{l}(f|x)|.$$

A second measure, which in our case is more discriminating, is the log pointwise predictive density (LPPD). This returns the average log probability assigned by the model to the correct label, given as,

$$\frac{1}{|\mathcal{Y}_{\text{test}}|} \sum_{(f,l) \in \mathcal{Y}_{\text{test}}} \log g(l|f, x).$$

Indeed, by Kuntz et al. [35], assuming that the data generating process produces independent samples, then this metric approximates the difference of the Kullback-Leibler divergence and the entropy of the data generating process. Indeed, the LPPD approximates

$$\begin{aligned} \int \log g(l|f, x) p(\mathrm{d}l, \mathrm{d}f) &= \int \int \log \left(\frac{g(l|f)}{p(l|f)} \right) p(\mathrm{d}l|\mathrm{d}f) p(\mathrm{d}f) + \int \log p(l|f) p(\mathrm{d}l, \mathrm{d}f) \\ &= - \int \mathrm{KL}(g(\cdot|f) \| p(\cdot|f)) p(\mathrm{d}f) + \int \log p(l|f) p(\mathrm{d}l, \mathrm{d}f), \end{aligned}$$

where $p(l, f)$ is the density from which the data is independently sampled. Hence, the larger the LPPD, the smaller the Kullback-Leibler divergence between our estimate and the true distribution.